

FEMA Region I Coastal Erosion Study – Nantucket County

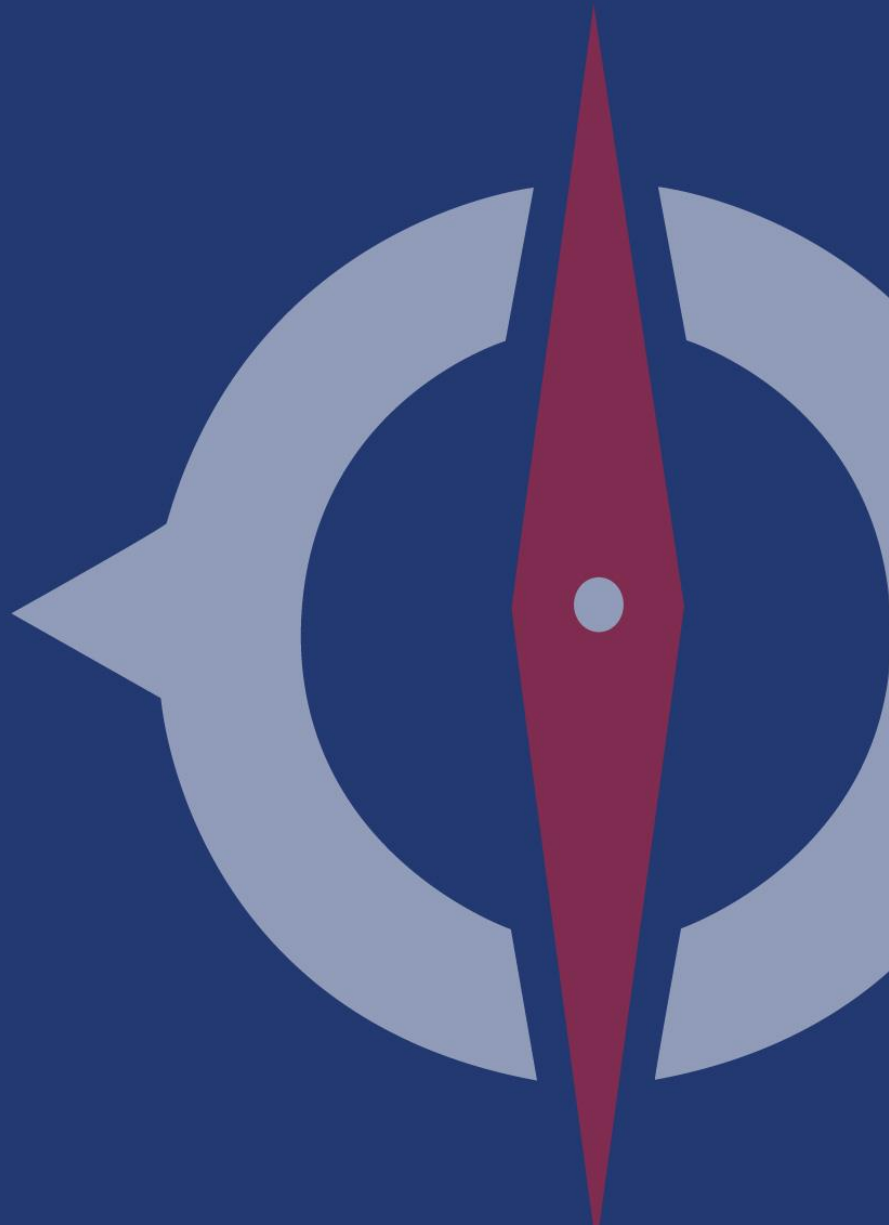
September 3, 2019

Prepared for:

**Federal Emergency Management Agency
US Department of Homeland Security
FEMA Region I**

Submitted by:

**Compass PTS JV
a JV led by AECOM and CDM Smith
3101 Wilson Boulevard, Suite 900
Arlington, VA 22201**



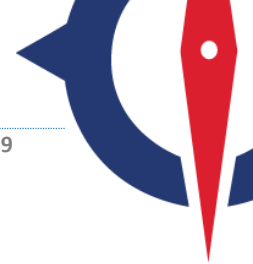


Table of Contents

01 Introduction	1
1.1 Study Purpose	1
1.2 Technical Study Elements	2
1.3 Study Area	3
02 Technical Approach	6
2.1 General Technical Approach	6
2.2 Analysis of Current Bathymetric and Topographic Data	9
2.3 Coastal Shoretypes	10
2.3.1 Sandy Dunes	10
2.3.2 Sandy Beaches	11
2.3.3 Coastal Bluffs	13
2.4 Determination of Historical Shoreline Change Trends	14
2.4.1 Historical Data	14
2.4.2 Sandy Beaches and Dunes	15
2.4.3 Coastal Bluffs	18
2.4.4 Linear Regression Rates (LRR)	19
2.4.5 Length of Historical Record	20
2.5 Sea Level Rise	23
2.5.1 Relative Sea Level Rise	24
2.5.2 Future Sea Level Rise Factors	26
2.6 Future Erosion Calculations	28
2.6.1 Sandy Dunes and Beaches	28
2.6.2 Coastal Bluffs	30
2.6.3 Hybrid Areas – Sandy Beaches Backed by Coastal Bluffs	31
2.6.4 The Bruun Slope	34
2.7 Field Site Visits	35
03 Results	37
3.1 Predicted Future Erosion	37
3.2 Coastal Erosion Hazard Area Maps	38
3.3 Mapping	40
04 Summary and General Recommendations	41
05 References	43



List Figures

Figure 1. An example of rapid coastal bluff erosion along Tom Nevers Beach on the southeastern side of Nantucket Island, Massachusetts..	1
Figure 2. The Study included the entire open coast shoreline of Nantucket Island.	4
Figure 3. An example of a sandy beach backed by dunes near Sesachacha Pond on the eastern shoreline of Nantucket Island, Massachusetts	5
Figure 4. An example of a wide sandy beach at the southern end of Siasconset on Nantucket Island, Massachusetts..	5
Figure 5. An example of a narrow sandy beach backed by a tall coastal bluff along Tom Nevers Beach on the southern shoreline of Nantucket Island, Massachusetts..	6
Figure 6. A general workflow diagram outlining the technical analysis steps.....	7
Figure 7. An example of a transect layout from the Nantucket study area..	8
Figure 8. An example of a cross-shore topographic profile extracted along a 1-D transect line..	10
Figure 9. An example of a sandy coastal dune from the beach near Sesachacha Pond on the eastern shoreline of Nantucket Island, Massachusetts.	11
Figure 10. An example of a wide sandy beach from the southeastern shore of Nantucket, Massachusetts. The beach is wide and flat. There is no dune present although there is a small, vegetated scarp (red line) that defines the active coastal erosion boundary..	12
Figure 11. An example of a transition area between well-defined coastal dunes and sandy beaches with small dune hummocks at a sandy spit between Westerly to Charleston, Rhode Island.	13
Figure 12. An example of a coastal bluff along Tom Nevers Beach on the southern shoreline of Nantucket Island, Massachusetts.	14
Figure 13. A conceptual diagram of the comparison between HWL shorelines, derived from aerial photographs, T-sheets, or beach surveys, and MHW.....	16
Figure 14. A rose plot of wave heights and directions for the years 2009 – 2017 from the NOAA NDBC Nantucket Sound Buoy (#44020).	17
Figure 15. An example of how MHW was found statistically on cross-shore profiles of sandy beaches and dunes.....	18
Figure 16. An example of a georeferenced historical aerial photograph of the southeastern Nantucket, Massachusetts shoreline near Tom Nevers Beach from 1969..	19
Figure 17. An example of an LRR calculated at a sandy beach transect on the eastern shore of Nantucket, Massachusetts.	20
Figure 18. Historical shoreline change rates (negative = accretion, positive = erosion) for transects along Nantucket, Massachusetts.....	21
Figure 19. Historical bluff erosion rates (positive = erosion) for two reaches along Nantucket, Massachusetts.	22
Figure 20. An example of an LRR determined at a transect placed along a bluff-backed beach near Tom Nevers Beach along the south shore of Nantucket, Massachusetts.	23
Figure 21. Future global SLR projections developed by Paris et al. (2012).	24
Figure 22. An example of relative SLR projections for a section of coastline from Westerly to Charleston, Rhode Island.....	25
Figure 23. An example of how the SLR factors (F) are calculated for the stretch of coast from Westerly to Charleston, Rhode Island.	27
Figure 24. A conceptual sketch of the predicted future erosion response at sandy dune and beach transects.....	29
Figure 25. A conceptual sketch of the predicted future erosion response at coastal bluffs.....	31

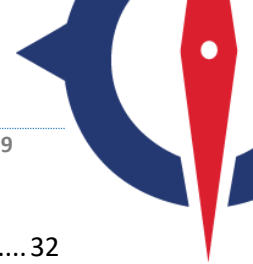


Figure 26. An example of a wide sandy beach backed by a coastal bluff at Siasconset, on the eastern shore of Nantucket, Massachusetts..	32
Figure 27. A conceptual diagram of the hybrid approach applied at eroding sandy beaches backed by stable coastal bluffs that are predicted to erode in the future.	33
Figure 28. An example of historical bluff erosion rates (LRRs) for transects in Nantucket, Massachusetts.	33
Figure 29. A conceptual diagram of how the Bruun Rule is typically applied with the Bruun slope (s) to the DOC.	34
Figure 30. An example of a cross-shore profile that reaches the DOC of -15 meters NAVD88 in two offshore locations, due to the presence of an offshore sand bar.	35
Figure 31. Compass conducted field site visits at Nantucket, Massachusetts from September 18 – 19, 2017.	36
Figure 32. The predicted future erosion distances under the Intermediate-High SLR scenario for the years 2030 (in yellow), 2050 (in red), and 2100 (in purple) along the south coast of Nantucket Island, near the airport.	38
Figure 33. An example of the mapped Intermediate-High SLR erosion scenarios for the southern shore of Nantucket, Massachusetts.	39
Figure 34. An example of an area where the future erosion predictions were modified in mapping at a coastal protection structure..	41

List of Tables

Table 1. Summary of Recently Collected Bathymetric and Topographic Data Sets.	9
Table 2. Historical Shoreline and Bluff Edge Data used to Determine Historical Shoreline Change Trends.	15
Table 3. MHW and MHHW Elevations used in the Technical Analysis at Each Site	18
Table 4. Acceleration Coefficients (b) for Future Sea Level Rise Scenario Curves from Paris et al. (2012).	24
Table 5. Observed Rates of SLR from Tide Gauges for Determining Future Relative SLR	25
Table 6. Predicted Relative Future SLR at Each Site for all Pilot Study Timeframes.	26
Table 7. Calculated Factors of Increase in Future SLR Rates Relative to Observed SLR Rates.	28



List of Acronyms

DEM	Digital Elevation Model
DOC	Depth of Closure
EPR	Endpoint Rate
ESRI	Environmental Systems Research Institute
FEMA	Federal Emergency Management Agency
FIMA	Federal Insurance and Mitigation Administration
FIRM	Flood Insurance Rate Map
LiDAR	Light Detection and Ranging
LRR	Linear Regression Rate
GIS	Geographic Information Systems
MHHW	Mean Higher High Water
MHW	Mean High Water
NAVD88	North American Vertical Datum of 1988 (NAVD88)
NOAA	National Oceanographic and Atmospheric Administration
NPF	Natural Protective Feature
NYDEC	New York Department of Environmental Conservation
SFHA	Special Flood Hazard Area
SLR	Sea Level Rise
TWL	Total Water Level
USGS	U.S. Geological Survey



01 Introduction

Coastal erosion is a hazard that threatens lives, property, and resources along much of the US coastlines (Figure 1). Erosion is generally expected to accelerate due to future sea level rise (SLR), putting more areas at risk (TMAC 2015). To help address the risk that this poses to communities, Compass has completed a Study, funded by the Federal Emergency Management Agency (FEMA) Region I, to investigate future coastal erosion due to SLR and produce future coastal erosion hazard maps. These maps consider multiple SLR scenarios and future timeframes to provide stakeholders with information to plan mitigation actions and build resilience in the face of a changing climate. The technical analysis and mapping were initiated in a Pilot Study of distinct shorelines in Massachusetts, Rhode Island, and New Hampshire. After completion of the Pilot Study, the technical analysis and mapping were expanded to other areas of Region I. This report summarizes the overall purpose of this Study and the technical methodology and the findings for Nantucket County. The maps are recommended as non-regulatory products to be used by communities as a tool to identify areas where coastal erosion is a hazard, plan future mitigation actions and ultimately facilitate the reduction of future erosion risk.



Figure 1. An example of rapid coastal bluff erosion along Tom Nevers Beach on the southeastern side of Nantucket Island, Massachusetts. Historical coastal bluff erosion has destroyed homes, roads, and other resources in this area.

1.1 Study Purpose

The general purpose of this Study was to develop future coastal erosion hazard area maps for Nantucket Island. Compass applied a technical methodology, developed in a previous Pilot Study of sections of coastline in Massachusetts, Rhode Island, and New Hampshire, to analyze historical trends in shoreline change, evaluate multiple future SLR projections and timeframes, estimate future erosion rates,



produce Flood Risk (i.e., non-regulatory) maps of future coastal erosion hazard areas, and synthesize a technical approach that could be expanded to other areas (Compass 2017). The overall Study and maps also meet several detailed objectives and fulfill multiple critical needs. Most importantly, there is a need for coastal communities to understand their risk from future SLR. Currently, FEMA Flood Insurance Rate Maps (FIRMs) only show the current flood risk to the 1-percent-annual chance coastal storm event for each particular area of the coast. They do not account for future SLR or long-term coastal erosion. Therefore, they are missing key information on a significant coastal hazard. Many communities look to FEMA as an authority on flood risk due to extreme coastal storms and it makes sense that FEMA would provide information on risks due to SLR. During some public meetings, community members have requested that FEMA investigate SLR and provide information on mapping products

The Study and maps also meet multiple agency goals. In 2017, The Federal Insurance and Mitigation Administration (FIMA) began proposing two “moonshots” for the future. These ambitious goals include doubling the amount of insurance policies and quadrupling the amount of mitigation actions by the year 2023. Furthermore, the Technical Mapping Advisory Council (TMAC) recently completed a study and found that future coastal erosion and SLR most likely pose a significant risk to homeowners (TMAC 2015). The final report made recommendations that FEMA provide Flood Risk products with information on future conditions, specifically SLR and coastal erosion. Finally, the Heinz Center completed a study also concluding that coastal erosion posed a significant risk to communities and had a significant negative impact on the National Flood Insurance Program (NFIP), and recommending that FEMA begin to investigate coastal erosion (Heinz Center 2000). This Study can help meet all of these agency goals and recommendations.

Finally, the Study and maps meet several technical objectives. In terms of size and scope, no similar studies of future coastal erosion due to SLR have been completed in the New England area. Although different agencies have investigated future coastal flooding and inundation due to SLR, none have addressed the related but distinct hazard of future shoreline retreat. This is important to highlight because there are several communities at relatively high coastal bluff elevations that are not directly vulnerable to future coastal flooding per se, but are directly vulnerable to future coastal bluff retreat. Investigating only future flooding due to SLR most likely underestimates the risk that these communities face. There have also been investigations into future shoreline change, but these rely on historical rates of erosion and do not incorporate the effects of future SLR. SLR is widely expected to accelerate coastal erosion and excluding this component most likely underestimates the risks. This Study presented an opportunity for FEMA to develop and apply a study methodology that incorporates these aspects and that can be expanded to other Regions. STARRII (2017) provided a review of SLR pilot studies conducted for FEMA in other regions. This Study also meets several specific TMAC technical recommendations (discussed later in this technical report).

1.2 Technical Study Elements

Compass filled in several technical gaps to develop a new methodology that is technically sound and applicable to the remaining Region I shoreline. These aspects are summarized in some detail in Section 2 (Technical Methodology), presented in full detail in the Pilot Study Report (Compass 2017), and are briefly listed here:

Sea Level Rise: The Study produced future coastal erosion hazard areas that account for historical trends in shoreline change and also account for future projections of SLR. The Study uses the National Oceanic



and Atmospheric Administration (NOAA) SLR projections, developed in 2012, as recommended by TMAC (2015). The global SLR projections were adjusted for local conditions.

Multiple Timeframes: The Study incorporated multiple future time frames (2030, 2050, and 2100) to meet the needs of different community members. Shorter timeframes (2030 and 2050) were included to be of use to current home mortgage holders and longer timeframes (2100) were included to be of use to community planners and engineers.

Coastal Bluff Erosion: In addition to sandy beach and dune erosion, the Study analyzed and predicted future rates of coastal bluff erosion. This is critical as several communities, particularly in Nantucket, Massachusetts, have been developed on tall coastal bluffs. Structures and lands within these communities will not be threatened by flooding due to future SLR, but will be vulnerable to bluff retreat due to future SLR.

Historical Shoreline Change Datasets: Compass analyzed historical (i.e., observed) rates of shoreline change at sandy dunes, beaches, and coastal bluffs. Instead of a simple endpoint rate (EPR) calculation, which consists of determining the distance between two historical shorelines or bluff edges and using the time between surveys to calculate a rate, Compass used multiple historical data points to determine linear regression rates (LRRs). LRRs take more data into account, reduce the impacts of historical outlier shoreline change events (such as extreme storms or beach nourishments), and are more accurate for long-term trends (Crowell et al. 1997; Crowell and Leatherman 1999; Hapke et al. 2010). In addition, Compass utilized all available historical shoreline and bluff edge data available (from the mid-1800's to 2010). This added more data points, reduced noisy alongshore variability in erosion rates, increased statistical confidence, and captured long-term trends.

Hybrid Erosion Analysis: Compass applied different erosion models at sandy shorelines (e.g., dunes and beaches) and bluff-backed shorelines. These two classes of shoretypes have different geomorphologies and are expected to respond differently to future SLR. After reviewing preliminary mapping, Compass determined that a hybrid erosion model was necessary at coastal bluffs fronted by a wide sandy beach. Siasconset Beach on Nantucket Island is an example of one of these areas. At Siasconset, there are areas to the north of rapid bluff erosion and areas to the south where the beach is eroding but the bluffs have historically been stable. Applying the beach erosion model to these stable bluff areas did not account for the fact that the bluffs, in the future, would not erode more slowly than a sandy beach. Compass developed a hybrid erosion model with Study SMEs.

1.3 Study Area

The initial Pilot Study areas offered a wide-variety of geomorphological conditions and the opportunity to develop a sound technical approach for different shoretypes. The shoreline geomorphologies included eroding sandy dunes and beaches, accreting sandy dunes and beaches, and eroding coastal bluffs. The Nantucket Study site includes the entire open coast shoreline of the island (Figure 2). Many areas are developed. The western, southern, and northern shorelines are similar and generally consist of narrow beaches backed by tall, rapidly eroding coastal bluffs or dunes. There are isolated sandy beaches that have historically accreted. The northeastern shoreline consists of a narrow, dynamic sandy spit with little development.

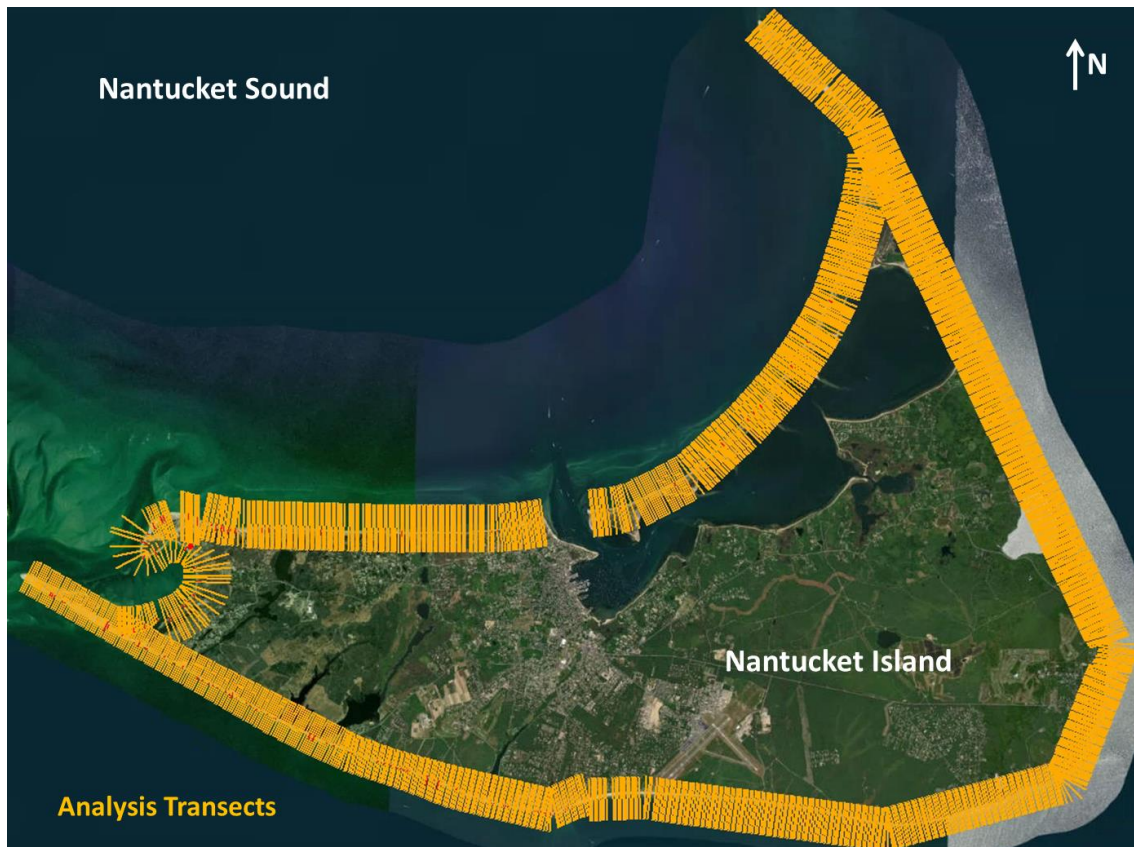


Figure 2. The Study included the entire open coast shoreline of Nantucket Island.

Within the Study area a variety of specific shoretypes were identified: sandy dunes (Figure 3), sandy beaches (Figure 4), and coastal bluffs (Figure 5).



Figure 3. An example of a sandy beach backed by dunes near Sesachacha Pond on the eastern shoreline of Nantucket Island, Massachusetts. The coastal dunes in this area are tall, well-formed, and vegetated.



Figure 4. An example of a wide sandy beach at the southern end of Siasconset on Nantucket Island, Massachusetts. The beach has historically accreted and has no well-formed sand dunes. The beach has a low vegetated ridge but no tall, well-formed sand dune.



Figure 5. An example of a narrow sandy beach backed by a tall coastal bluff along Tom Nevers Beach on the southern shoreline of Nantucket Island, Massachusetts. The beaches and bluffs in this area have historically eroded.

02 Technical Approach

This section provides details on the technical approach developed and applied to determine the historical trends in shoreline change and predict future shoreline change due to SLR.

2.1 General Technical Approach

As the technical approach consisted of many steps, this section provides a general outline. A workflow diagram is presented in Figure 6. Details on each step are presented in the following sections.

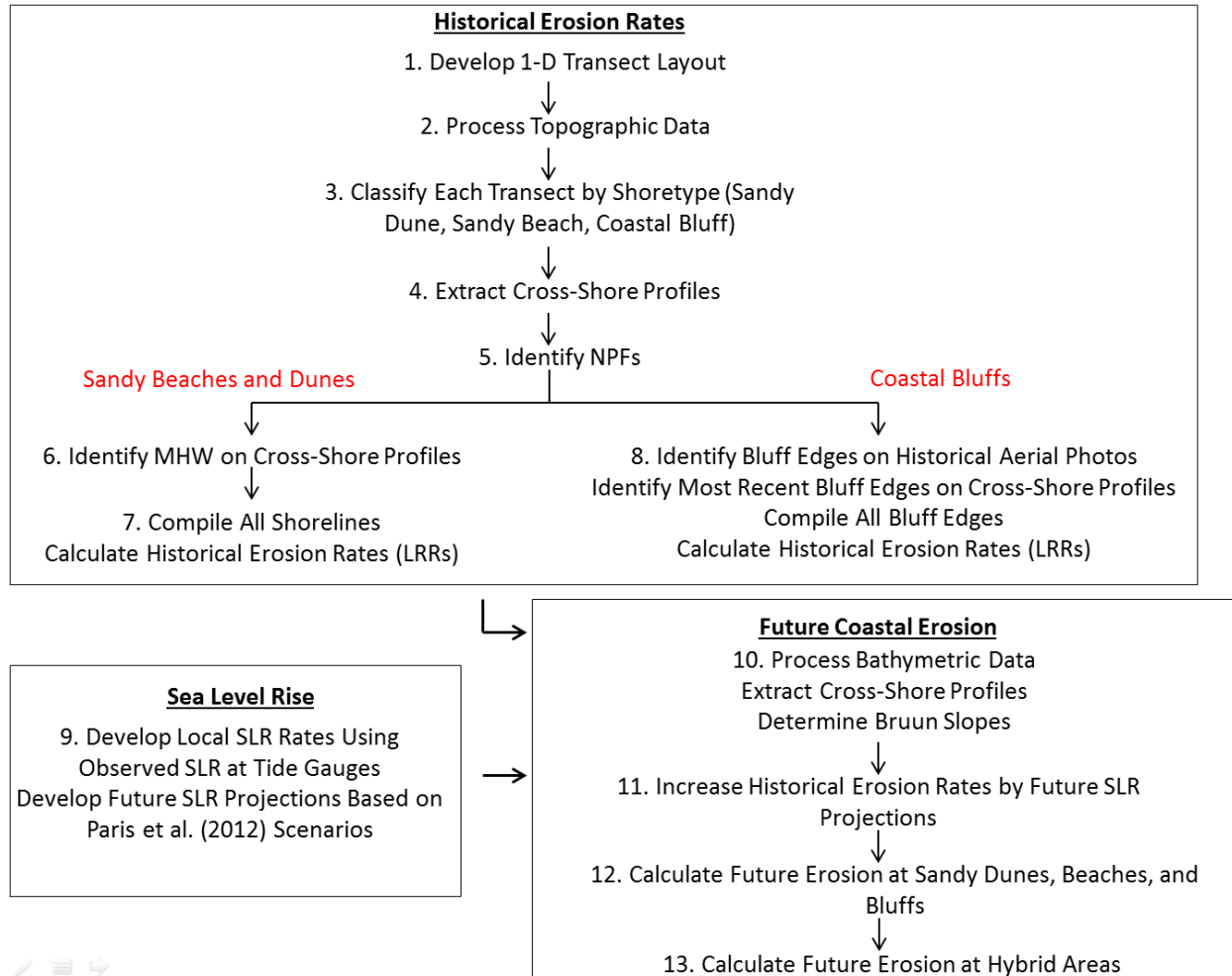


Figure 6. A general workflow diagram outlining the technical analysis steps.

1. Compass implemented a one-dimensional (1-D) transect-based approach, where transects were placed approximately every 50 meters and oriented perpendicular to the shoreline (Figure 7). All analysis and calculations were done along each transect. Compass initially began with the transect layout developed by Hapke et al. (2010) for the USGS National Assessment of Shoreline Change in areas where this previous study had been completed. In areas with no USGS transect layout, Compass placed new transects. After initial placement, transects were then shifted, oriented, added, and removed to suit the specific needs of this Study.
2. Recently collected topographic light detection and ranging (LiDAR) data sets were downloaded and processed for each site. These were used to establish current coastline conditions and provide a baseline for future erosion projections.
3. The transects were classified by shore type based on the shoreline geomorphology (sandy beach, sandy dune, and coastal bluff) using aerial images, a digital elevation model (DEM) developed from the airborne topographic LiDAR data, and field site visits.

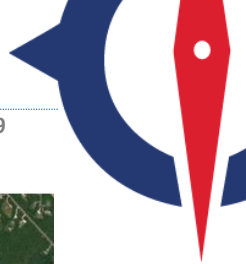


Figure 7. An example of a transect layout from the Nantucket study area. For this Study, Compass followed the same approach and implemented a one-dimensional (1-D) transect-based approach, where transects were placed approximately every 50 meters and oriented perpendicular to the shoreline.

4. Cross-shore profiles were extracted from the topographic LiDAR data along each transect line.
5. To establish a baseline to project future erosion hazard zones from, the current natural protective feature (NPF) was identified on each cross-shore profile. NPFs consisted of beach scarps, dune crests, or bluff edges depending on shoretype.
6. Mean high water (MHW) was identified on each cross-shore profile.
7. At sandy beaches and dunes, historical shoreline data was compiled from Hapke et al. (2010) and the Massachusetts Office of Coastal Zone Management (CZM). These historical shoreline data points were combined with MHW points to calculate historical shoreline change rates (LRRs) for each transect.
8. At bluff-backed beaches, historical bluff edges were identified from georeferenced historical aerial photos at each transect. The most recent bluff edge was identified on each cross-shore profile and combined with the historical bluff edges to calculate historical shoreline change.
9. Global SLR projections developed by NOAA in 2012 (Paris et al. 2012) were adjusted using local rates of SLR observed at tide gauges near each site.
10. Recently collected bathymetric data sets were downloaded and processed for each site. Cross-shore profiles were extracted from the bathymetry data and were used to determine nearshore profile slopes (Bruun slopes) used for future erosion projections with SLR.
11. The local relative rates of SLR and future projections of SLR were then used to adjust the historical rates of shoreline change (LRRs) and project future shoreline change.
12. The technical approach applied at sandy beaches, dunes, and coastal bluffs was used from the FEMA Region IX Pilot Study (BakerAECOM 2016).
13. Compass developed and applied a hybrid erosion model to predict future erosion at sandy beaches backed by erodible coastal bluffs that are currently stable.



Mapped future erosion hazard areas were created based upon four NOAA SLR scenarios (Low, Intermediate-Low, Intermediate-High, and High) over three future time frames (the years 2030, 2050, and 2100).

2.2 Analysis of Current Bathymetric and Topographic Data

The first step in the technical analysis was to obtain and process recently collected bathymetric and topographic data. Recently collected bathymetric sets data were necessary to calculate nearshore profile slopes (Bruun slopes), which are used in future erosion projections with SLR. Recently collected topographic data were required to identify the current NPFs (beach scarps, dune crests, or bluff edges), MHW at sandy beach and dune transects, and to calculate historical rates of change. The topographic data sets were particularly important because they established the baseline shoreline conditions for projecting long-term future shoreline change. To predict long-term future shoreline change, it is critical that the topographic data be representative of typical shoreline conditions, and not representative of recent episodic shoreline change events, including large coastal storms or nourishment projects (Crowell et al. 1997; Crowell and Leatherman 1999). In 2012, Superstorm Sandy eroded several sandy beaches within Region I and there were multiple post-storm airborne topographic LiDAR surveys of the coast. Many of these beaches were temporarily eroded and may recover so that post-storm surveys are likely not representative of long-term shoreline change. Therefore, Compass identified and used topographic 2010 LiDAR that was recent, but not collected after Superstorm Sandy.

Table 1 summarizes the bathymetric and topographic data sets analyzed in this Study area. All airborne topographic LiDAR data were collected in 2010. These data established the baseline shoreline conditions for future erosion calculations. It is important to clarify that even though the data were not collected at the time of this study, the projections of future erosion are valid and will still be valid in the future. This is because 2010 was also taken as the baseline year for projections future erosion to 2030, 2050, and 2100. Theoretically, the Study could be repeated in the future with a new baseline year and topographic data and the same results would be achieved, if shoreline change trends continue as forecasted. For bathymetry data, it is not known if the USGS Topobathymetric DEMs include post-Superstorm Sandy bathymetric data; however, it is likely they do not as all source hydrographic survey data cited in the included metadata was older than 2012.

Table 1. Summary of Recently Collected Bathymetric and Topographic Data Sets.

County	Bathymetric Data	Topographic Data
Nantucket County	USGS Topobathymetric DEM 1887 - 2016	2010 FEMA Airborne Topographic LiDAR

Note: All data are publically available and were obtained from NOAA's Digital Coast Website:
<https://www.coast.noaa.gov/digitalcoast/>

All bathymetric and topographic data were processed and analyzed in Universal Transverse Mercator (UTM) Zone 19 coordinates and relative to the North American Vertical Datum of 1988 (NAVD88). Cross-shore profiles were extracted from the topographic data along each transect (Figure 8).

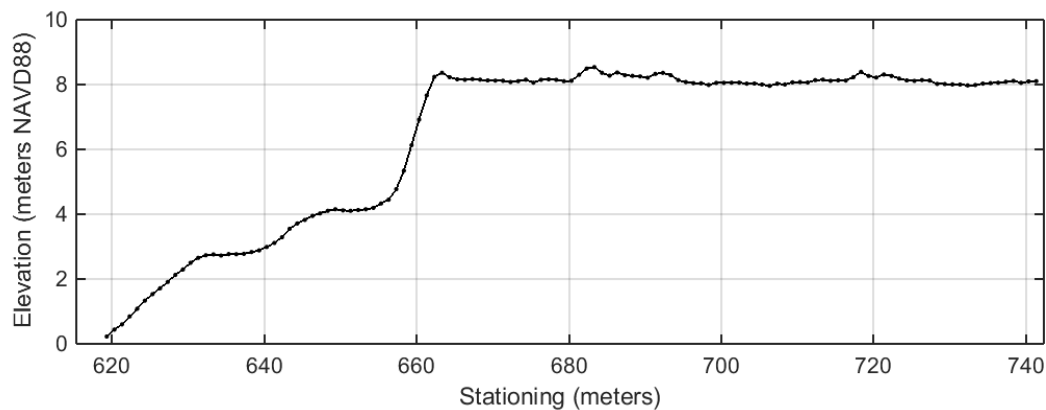


Figure 8. An example of a cross-shore topographic profile extracted along a 1-D transect line. Cross-shore profiles were extracted in meters horizontally and meters relative to NAVD88 vertically.

2.3 Coastal Shoretypes

Once cross-shore topographic profiles were extracted along each transect, they were classified by shoretype (sandy dunes, sandy beaches, and coastal bluffs). Each shoretype was defined following a framework detailed in the following sections. The purpose of this step was to establish the type of future erosion response at each transect (sandy shoreline versus erodible bluff). Once the shoretype was defined for a particular transect, the NPF (dune crest, beach ridge, or bluff edge) was identified on each cross-shore profile. The NPF is the current active natural barrier to coastal erosion during typical conditions. The purpose of identifying the NPF on each transect was to establish the baseline for future erosion projections on the transect. In later stages during the final mapping, the NPFs along all transects were mapped as the current coastal boundary. Both the shoretype classification and NPF identification were completed visually using a combination of the cross-shore profile data, the DEM, publicly available current and historical aerial photographs, and field site visits. Details are provided in the following sections.

2.3.1 Sandy Dunes

For sandy shorelines (dunes and beaches), Compass generally defined the NPF as the approximate landward limit of the coastal total water levels (TWLs) over typical or average conditions (not during an extreme storm event). Coastal TWLs are the combination of astronomical tides, storm surge, wave setup, and wave runup, and are ultimately the driver for coastal erosion. The approximate landward limit of the TWL along each transect was not calculated, but estimated visually based on several aspects. These included the location of a beach scarp or dune ridge in the cross-shore profile and DEM, and the presence wrack lines and High Water Lines (HWLs) in aerial photos and field site visits. Each NPF is the current natural barrier along a transect to coastal erosion during typical conditions. Coastal erosion during an extreme storm might project far inland and does not establish an accurate baseline for future long-term shoreline change analysis. The landward limit of average coastal erosion is more representative of typical conditions and an accurate baseline for future long-term shoreline change analysis (Crowell et al. 1997; Crowell and Leatherman 1999; Hapke et al 2010).



Dunes were identified at sandy beaches backed by a well-formed, continuous sand dune with a clear geometry (i.e., easily identifiable dune toe, crest, and heel on the cross-shore profile) (Figure 9). For this Study, dunes were required to be at least two meters tall (from toe to crest) to distinguish between small dune hummocks and coastal foredunes. It was reasoned that coastal dunes should be tall enough to provide some short-term protection against coastal flooding. This criteria was simply used to avoid categorizing small dune hummocks as dunes and did not impact the analysis or mapping in the alongshore. The NPF was identified at the dune crest, which was nearly always vegetated. In some areas, the most seaward crest appeared as a ridge rather than a peak. On cross-shore profiles with multiple dune crests, the NPF was identified as the most seaward dune crest, to represent the current barrier to coastal erosion.

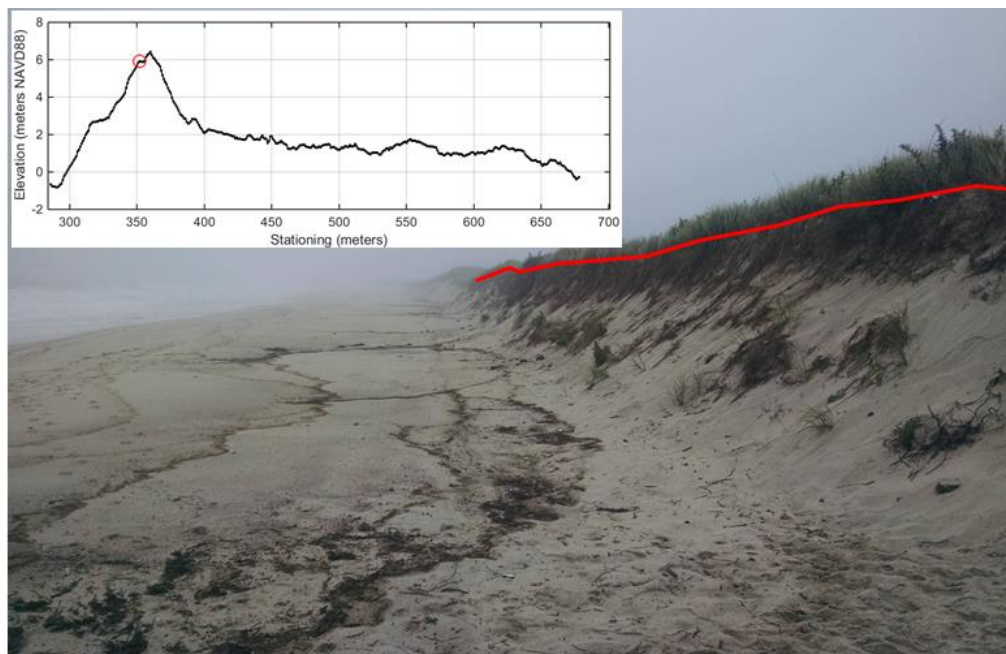


Figure 9. An example of a sandy coastal dune from the beach near Sesachacha Pond on the eastern shoreline of Nantucket Island, Massachusetts. The dune is well-defined and over two meters tall. The most seaward crest (red line) was identified as the NPF on a cross-shore profile from the site. In some areas, the most seaward crest appeared as a ridge rather than a peak. The wrack line in the photograph indicates that the vegetated dune ridge is the current boundary to coastal erosion and the TWL.

2.3.2 Sandy Beaches

Transects placed at wide sandy beaches with no well-defined coastal dunes were categorized as sandy beaches (Figure 10). These beaches were typically wide and flat, with a distinct scarp that delineated the active coastal erosion boundary. Often, the scarp was vegetated along the ridge. In some areas there were small dune hummocks that had not yet developed into continuous coastal dunes. At many sites these were less than one meter tall.

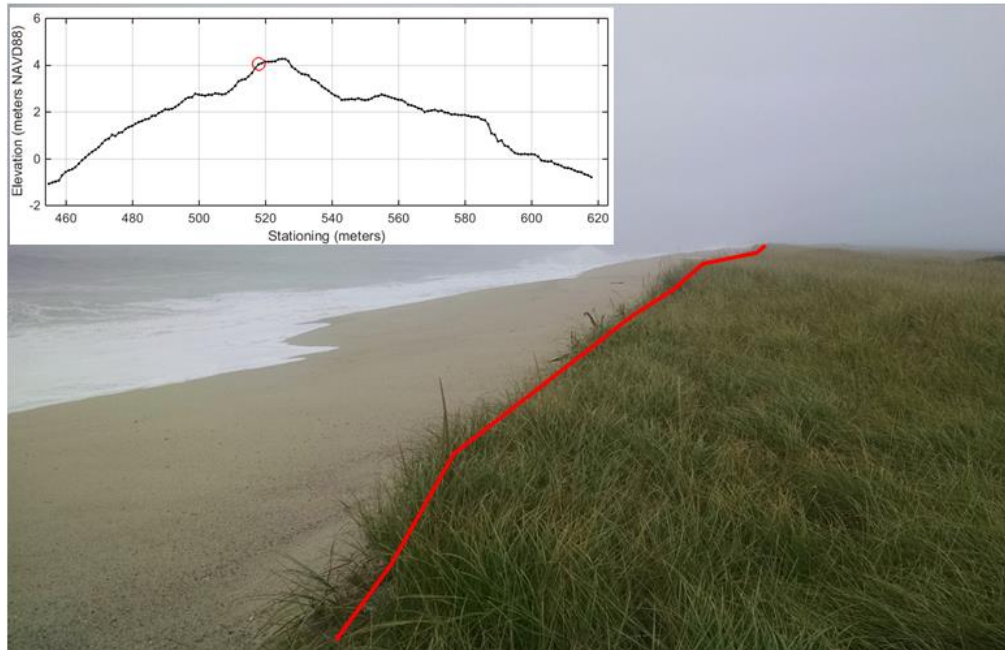


Figure 10. An example of a wide sandy beach from the southeastern shore of Nantucket, Massachusetts. The beach is wide and flat. There is no dune present although there is a small, vegetated scarp (red line) that defines the active coastal erosion boundary. The ridge at this scarp was identified as the NPF.

It is critical to highlight that the distinction between the dune and beach classification had no impact of the analysis or mapping in the alongshore. Both types of sandy shorelines were analyzed for future erosion in the same manner. Furthermore, in areas of transition between beaches and dunes, the beach ridge aligned with the most seaward dune crest in the alongshore and delineated the active coastal erosion boundary (Figure 11). Therefore, there was no transition between the NPFs and the mapped future erosion hazard areas. The shoretype classifications were adopted only to accurately categorize the existing shoreline geomorphology of each transect.

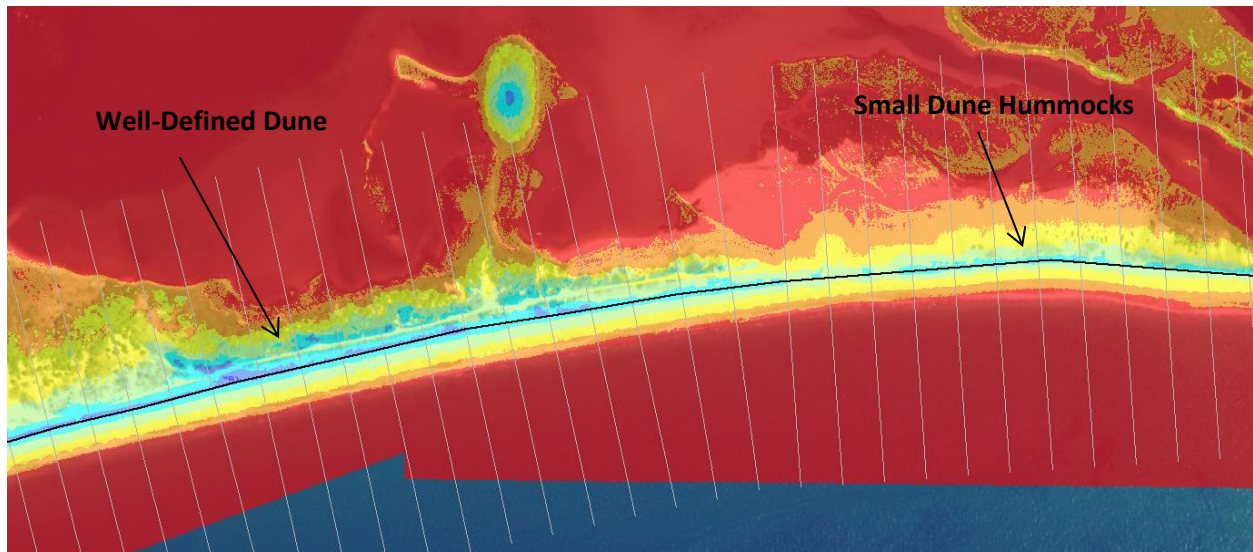
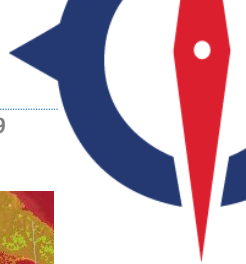


Figure 11. An example of a transition area between well-defined coastal dunes and sandy beaches with small dune hummocks at a sandy spit between Westerly to Charleston, Rhode Island. Analysis transects are shown in grey and the NPF line is shown in black. There are tall well-defined dunes to the left of the figure and small, segmented dune hummocks to the right. The most seaward dune crest aligned with the most beach ridge in the alongshore and delineated the active coastal erosion boundary, such that the change in shoretype classification had no impact on the analysis and mapping. The shoretype classifications were adopted only to accurately categorize the existing shoreline geomorphology of each transect.

2.3.3 Coastal Bluffs

Transects placed at actively eroding coastal bluffs were categorized as coastal bluffs (Figure 12). On each cross-shore profile, the bluff edge was selected as the NPF and active coastal erosion boundary.

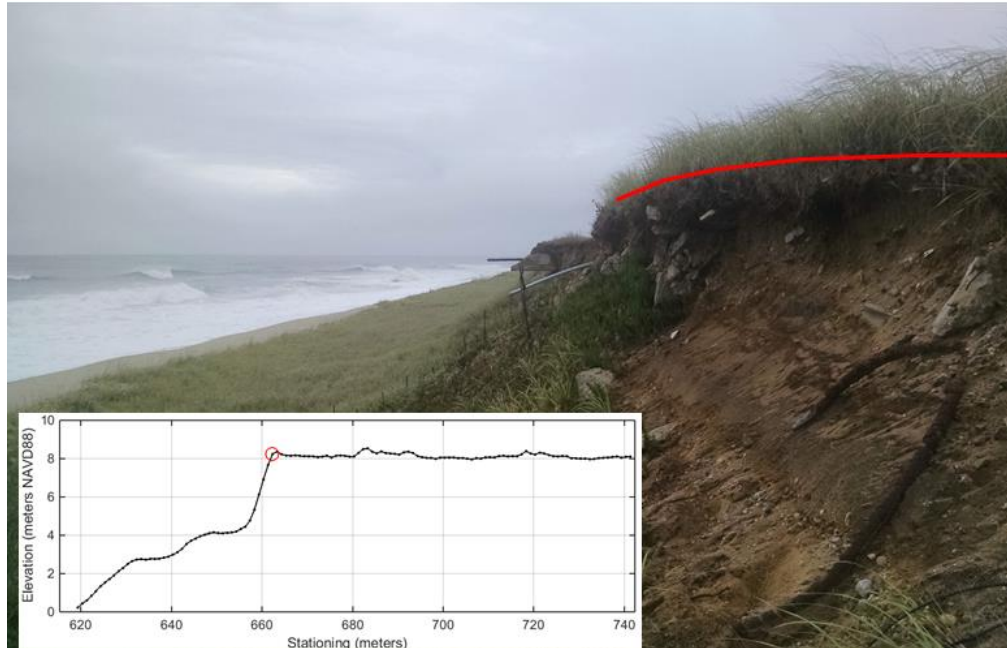


Figure 12. An example of a coastal bluff along Tom Nevers Beach on the southern shoreline of Nantucket Island, Massachusetts. The bluff edge (red line) was selected as the NPF and active coastal erosion boundary.

2.4 Determination of Historical Shoreline Change Trends

The section details the calculation of historical shoreline change trends. Historical shoreline data was used to calculate historical erosion or accretion rates of sandy beaches and dunes. Historical bluff edge data was used to calculate historical erosion rates of coastal bluffs.

2.4.1 Historical Data

Compass used some historical data to determine historical shoreline change rates. For sandy shorelines (dunes and beaches), Compass used historical shoreline data in GIS format from the USGS National Shoreline Assessment (Hapke et al. 2012) and the Massachusetts Office of CZM. Older data included historical shorelines derived from NOAA T-Sheets and from aerial photographs. These shorelines were delineated by visual identification of the high water line (HWL) during historical surveys or during the processing and analysis of the aerial photographs.

For coastal bluff areas, Compass used historical aerial photos of the coastline from the publically accessible USGS Earth Explorer. The historical bluff edges were visually identified on the aerial photos. More recent bluff edges were visually identified on each cross-shore profile extracted from the airborne topographic LiDAR data. Table 2 summarizes the historical data sets used in the Study.

**Table 2.** Historical Shoreline and Bluff Edge Data used to Determine Historical Shoreline Change Trends.

County	Historical Sandy Shoreline Data Year (Data Type)	Historical Coastal Bluff Edge Data Year (Data Type)
Nantucket County	1846 (HWL - NOAA T-Sheet) ^{1,4} 1887 (HWL - NOAA T-Sheet) ^{1,4} 1955 (HWL - Aerial Photograph) ^{1,4} 1978/79 (HWL - Aerial Photograph) ^{1,4} 1994 (HWL - Aerial Photograph) ^{1,4} 2000 (MHW - LiDAR) ^{1,4} 2010 (MHW - LiDAR) ³	1969 (Bluff Edge - Aerial Photograph) ² 1995 (Bluff Edge - Aerial Photograph) ² 2003 (Bluff Edge - Aerial Photograph) ² 2010 (Bluff Edge - LiDAR) ³

Notes: Data sources include 1 – USGS National Shoreline Assessment (Hapke et al. 2010); 2 – USGS Earth Explorer (<https://earthexplorer.usgs.gov/>); 3 – NOAA Digital Coast (<https://coast.noaa.gov/>); 4- Massachusetts CZM (http://maps.massgis.state.ma.us/map_ol/moris.php).

2.4.2 Sandy Beaches and Dunes

To calculate historical rates of shoreline change at sandy beaches and dunes, Compass compared historical HWLs derived from T-Sheets and aerial photographs to more recent MHW positions on LiDAR-derived cross-shore profiles. Many previous studies have utilized HWLs for shoreline change analysis (Crowell et al. 1993). Ruggiero (2009) found that when comparing HWLs from photos, T-Sheets, or beach surveys (proxy-based shorelines) to MHW (a tidal datum-based) shoreline, a correction needs to be applied for wave effects (Figure 13). This is necessary because visually identified HWLs include the effects of wave setup and wave runup, while the position of MHW is based on astronomical tides alone. On any given day, the HWL will be further inland than MHW because of wave setup and runup. The USGS Shoreline Change Assessment (Hapke et al. 2010) includes averaged correction factors for all historical HWL shorelines derived from T-Sheets and photos based on typical wave and beach slope conditions. In areas with USGS Shoreline Change Assessment data, Compass used these correction factors to adjust the historical HWL data.

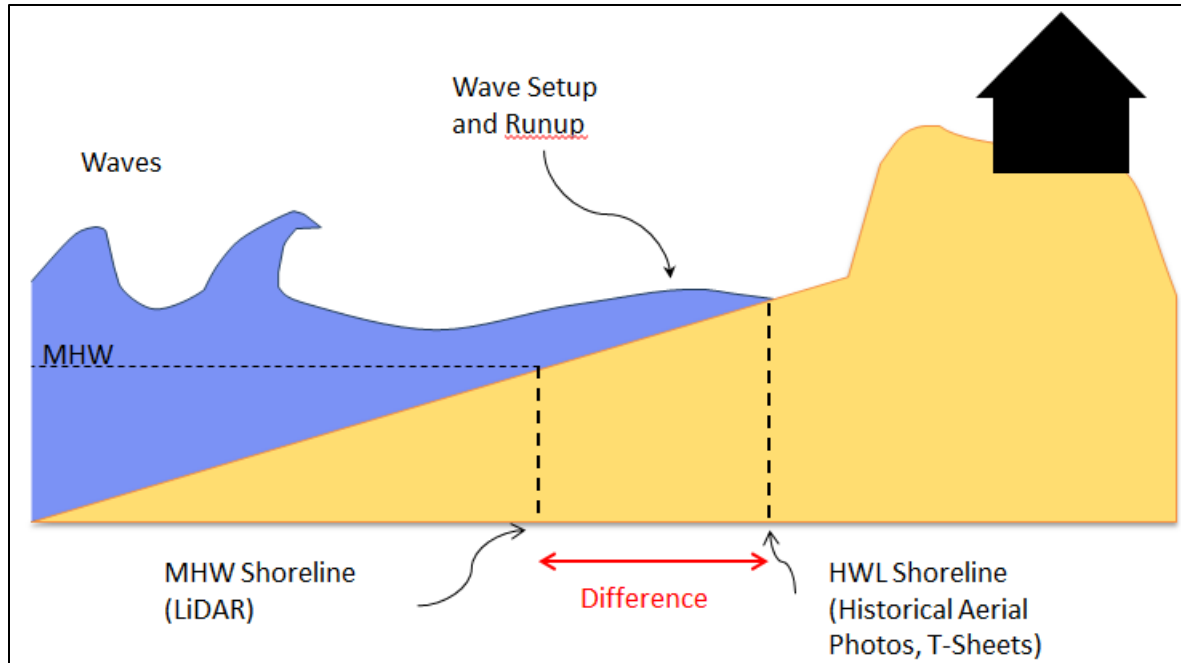


Figure 13. A conceptual diagram of the comparison between HWL shorelines, derived from aerial photographs, T-sheets, or beach surveys, and MHW. HWL shorelines include the effects of wave setup and wave runup while MHW is a tidal-based datum shoreline and includes the effects of astronomical tides only. The HWL shorelines were adjusting using correction factors from the USGS National Shoreline Assessment (Hapke et al. 2010).

In areas with no USGS shoreline change assessment data, including the northern and western coasts of Nantucket Island, Compass calculated correction factors following the USGS approach and using local wave and cross-shore profile data. Wave setup and runup heights are typically a function of wave height, wave period, and beach or coastal barrier slopes (Stockdon et al. 2006). For wave characteristics, Compass first obtained historical wave data from proximate NOAA National Data Buoy Center (NDBC) buoys (Figure 14). For slope characteristics, Compass calculated the beach slope within +/- one meter of MHW on each cross-shore profile derived from the 2010 LiDAR data. The correction factor for each transect was then obtained by calculating the height of wave setup and runup using the Stockdon et al. (2006) empirical formula, which is widely used in coastal studies:

$$Bias = R_{2\%}/\beta_f = 1.1 \left[0.35\beta_f\sqrt{H_0L_0} + \frac{\sqrt{[H_0L_0(0.563\beta_f^2 + 0.004)]}}{2} \right] \div \beta_f \quad (\text{Equation 1});$$

where $R_{2\%}$ is the two-percent exceedance wave setup and runup height, H_0 is the average deepwater significant wave height, L_0 is the average deepwater wave length, and β_f is the slope around MHW.

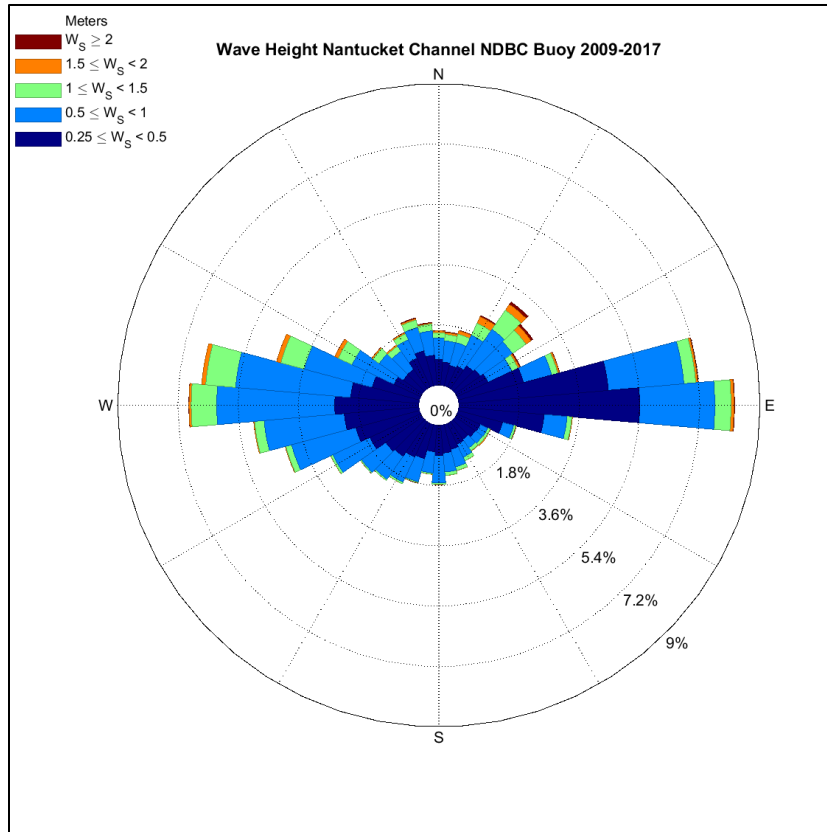


Figure 14. A rose plot of wave heights and directions for the years 2009 – 2017 from the NOAA NDBC Nantucket Sound Buoy (#44020). The plot is an example of the data that were used to calculate average wave heights and wave periods to estimate the correction factors between HWL and MHW in historical shoreline change analysis.

Compass added a more recent historical shoreline at each site from the 2010 airborne topographic LiDAR data (Table 2). The shoreline was found statistically by fitting a linear regression through profile data at each cross-shore profile around the MHW elevation, and then using the best fit linear regression equation to calculate the cross-shore position of MHW (Stockdon et al. 2002; Hapke et al. 2010). The technique is more accurate than simply visually identifying MHW on each cross-shore profile, particularly on flatter profiles with undulations near the shoreline. Table 3 summarizes the MHW elevations for each site. Weber et al. (2005) analyzed tide gauge data along several US coastlines and established MHW elevations for shoreline change analysis. Mean higher high water (MHHW) elevations were used to calculate the Bruun slopes in the future erosion analysis and are also presented in Table 3.

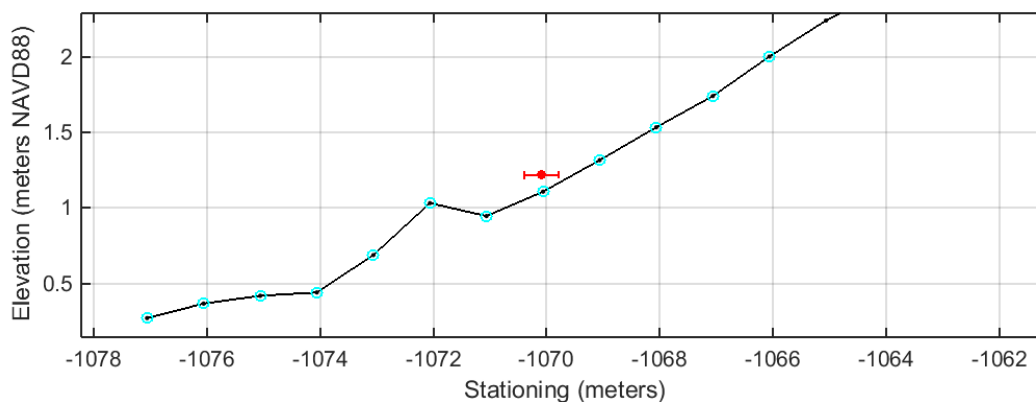


Figure 15. An example of how MHW was found statistically on cross-shore profiles of sandy beaches and dunes. A linear regression was fit to profile data within 1 meter of the MHW elevation (1.22 meters NAVD88 – turquoise circles) and the resulting best-fit equation was used to calculate the cross-shore position of MHW. The predicted MHW location is shown in red with 90 percent confidence intervals (red circle and bars). The approach was developed by Stockdon et al. (2002).

Table 3. MHW and MHHW Elevations used in the Technical Analysis at Each Site

County	Tidal Datum	Elevation (meters NAVD88)	Source
Nantucket County	MHW	0.29	Weber et al. (2005)
	MHHW	0.49	NOAA Station #8449130 ¹

Notes: 1 – Data available at <https://tidesandcurrents.noaa.gov/>

2.4.3 Coastal Bluffs

To calculate historical rates of shoreline change at coastal bluffs, Compass georeferenced historical aerial images (Table 2). The photos were georeferenced using Environmental Systems Research Institute (ESRI) GIS tools, following a procedure developed in the NYDEC study.



Figure 16. An example of a georeferenced historical aerial photograph of the southeastern Nantucket, Massachusetts shoreline near Tom Nevers Beach from 1969. The georeferenced historical aerial photograph was used to identify the historical bluff edge (red dashed line).

2.4.4 Linear Regression Rates (LRR)

In the Pilot Study, Compass performed an investigation to determine the most appropriate method to calculate historical shoreline change rates, ultimately selecting LRRs which are widely used in shoreline change analysis (Crowell et al. 1997; Crowell and Leatherman 1999; Hapke et al. 2010). LRRs are statistically determined by fitting a line through multiple historical shoreline data points. The slope of the best-fit line is the shoreline change rate (meters/year) (Figure 17). LRRs naturally incorporate more data points and are therefore less impacted by short-term variability in shoreline change and better suited to calculate long-term trends. For example, sandy beaches can go through seasonal and inter-annual periods of erosion and accretion. Even beaches that have been eroding in the long-term may have brief periods of accretion. Figure 17 illustrates an example of this from the eastern shore of Nantucket Massachusetts. Furthermore, by including additional shoreline data points, LRRs reduce the impacts of outlier points. Outlier points can be either erosional or accretionary, due to nourishments or storms, and they are not representative of long-term trends. Although Compass avoided more recent LiDAR survey data collected after Superstorm Sandy, we were unable to discern if any of the historical shorelines were outliers. Finally, LRRs also provide a degree of statistical confidence on the historical erosion or accretion rates, in the form of a 90 percent confidence interval. The confidence intervals can be incorporated into future erosion hazard areas.

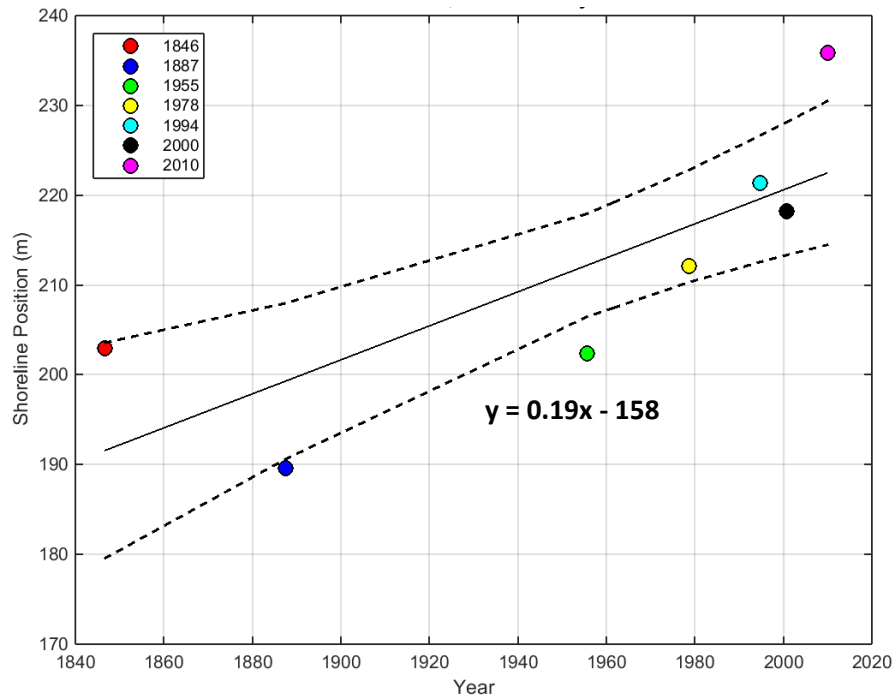


Figure 17. An example of an LRR calculated at a sandy beach transect on the eastern shore of Nantucket, Massachusetts. The black line is the best-fit trend line and the dashed lines represent the 90 percent confidence intervals. The slope of the line is the shoreline change rate (eroding 0.19 meters/year). Positive slope is erosion and negative slope is accretion. The best fit equation is displayed in the figure. The LRR takes into account multiple historical shorelines from 1846-2010.

2.4.5 Length of Historical Record

In the Pilot Study, Compass also performed an investigation to determine the length of historical record that was most appropriate for predictions of long-term future coastal erosion, ultimately selecting a relatively long timeframe from the mid-1800's – 2000's. Previous studies have shown that longer timeframes might be more representative of long-term trends if older historical data is available (Crowell et al. 1997; Crowell and Leatherman 1999; Hapke et al. 2010). These studies demonstrated how short-term shoreline change rates can be larger in magnitude and more variable. An example of the long-term historical rates for a portion of shoreline is shown in Figure 18.

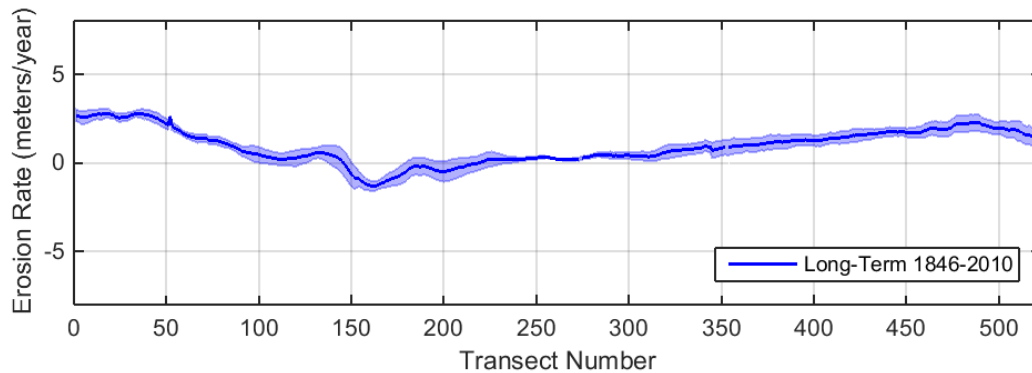


Figure 18. Historical shoreline change rates (negative = accretion, positive = erosion) for transects along Nantucket, Massachusetts. The top panel shows short-term rates (1978-2010) and the bottom panel shows long-term rates (1846-2010). The rates are shown in blue with 90 percent confidence intervals indicated by shading.

There are additional reasons for selecting a longer timeframe. Calculating historical shoreline change rates over longer timeframes allows for the inclusion of additional shoreline data points. This further reduces the impacts of outlier points in the calculation of LRRs as discussed in the previous section. In addition, Compass is predicting future erosion hazard areas based on 20, 40, and 90 year timeframes (using 2010 as a baseline year for the years 2030, 2050, and 2100). As most of these timeframes are longer than 30 years, it is reasonably consistent to calculate historical shoreline change over similar timeframes longer than 30 years (i.e., longer than 1978-2010). Finally, in subsequent steps of the technical analysis, Compass attributed some of the historical erosion to historical SLR measured at tide gauges. This was done for the determination of future erosion hazard areas and is detailed in following sections. SLR has been observed at the Battery, New York tide gauge since the mid 1800's and several other tide gauges on the Atlantic Coast since the early-1900's (Zervas et al. 2013). This indicates that SLR may have affected shoreline change since the mid-1800's and early 1900's. Therefore, it is reasonable to include historical shorelines from these earlier dates. For all of these reasons, a longer timeframes and use all available historical data at each site appears to be a better approach for this study (Table 2).

The same holds true for bluff-backed shorelines. Historical photographs dating back to 1969 were obtained for bluff backed beaches on Nantucket, Massachusetts (Table 2). No older photos of sufficient quality to be georeferenced and analyzed were available. 1969 – 2010 is a much shorter timeframe than the analyzed timeframes for sandy beaches and dunes; however, this is not expected to significantly impact the calculations of long-term bluff erosion. This is because the calculated bluff erosion rates have less variability compared to the sandy shoreline change rates, over similar timeframes (Figure 19). This is most likely because bluffs can only erode while beaches and dunes can both erode and prograde, making bluff change inherently less variable than sandy shoreline change over the long-term. An example of a LRR determined at bluff backed beach is shown in Figure 20.

At all sites and for all shoretypes (sandy and bluff), Compass decided to use all available historical data unless there was clear evidence that the data was not representative of long-term shoreline change trends.

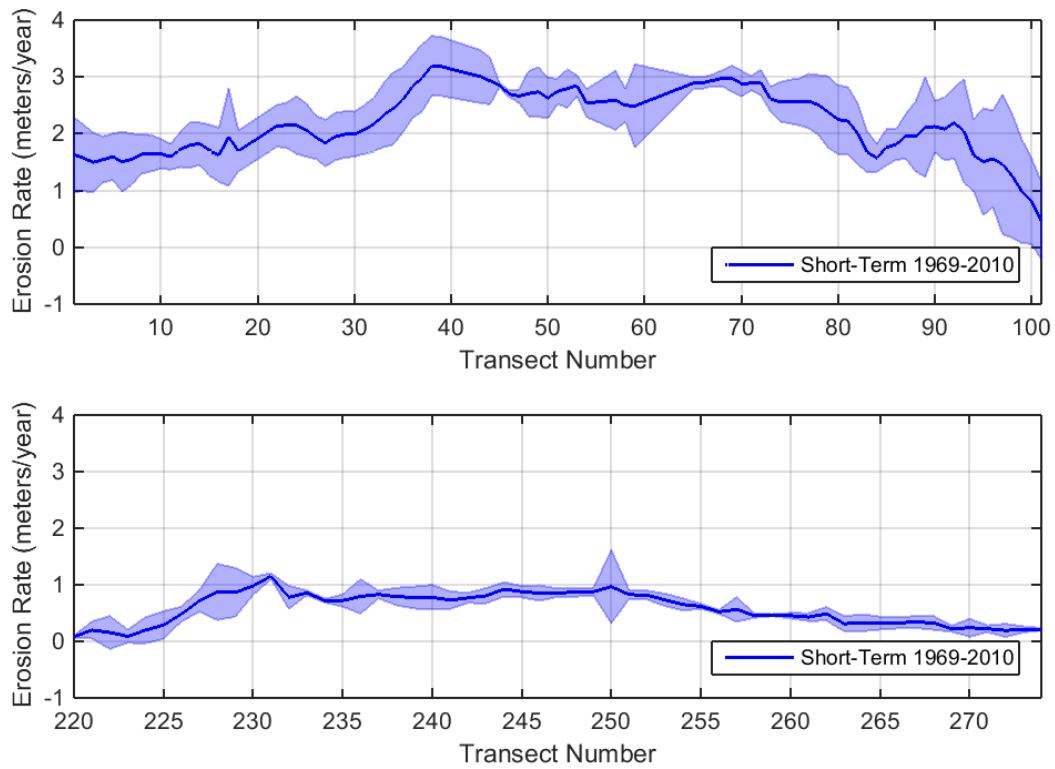


Figure 19. Historical bluff erosion rates (positive = erosion) for two reaches along Nantucket, Massachusetts. The rates are shown in blue with 90 percent confidence intervals indicated by shading. The alongshore variability is relatively small compared to sandy shoreline change rates.

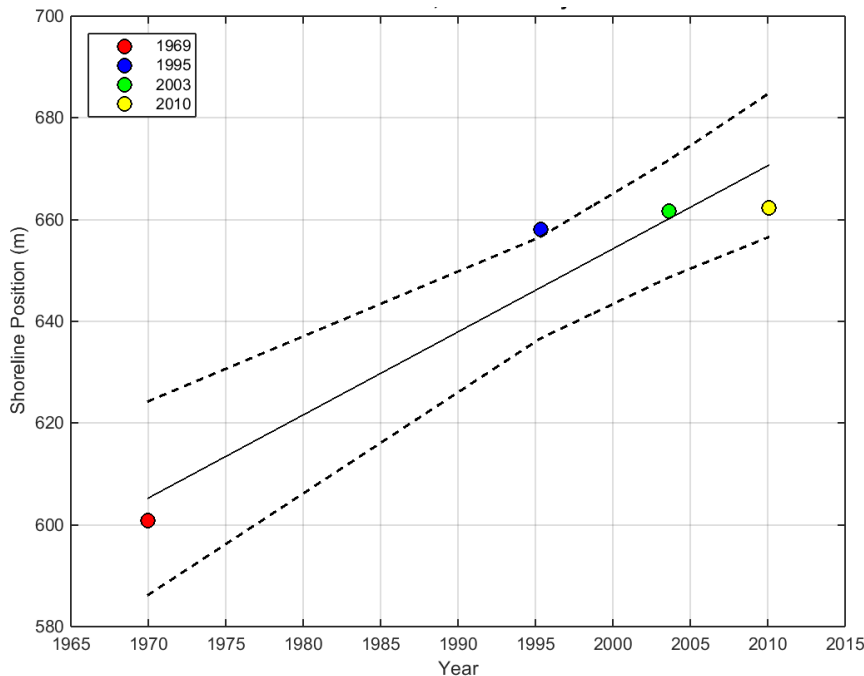


Figure 20. An example of an LRR determined at a transect placed along a bluff-backed beach near Tom Nevers Beach along the south shore of Nantucket, Massachusetts. The slope of the best-fit line, and historical erosion rate, is 1.63 meters/year.

2.5 Sea Level Rise

The Nantucket Study followed the TMAC (2015) recommendations to use future global SLR projections developed by Paris et al. (2012). There are four future global SLR scenarios (Figure 21) which vary based upon global greenhouse gas emissions scenarios. There is a considerable range in the future SLR predictions. The Low SLR scenario assumes that SLR increases at the observed rate (1.7 millimeters/year) and that there is no acceleration. The High SLR scenario predicts future SLR acceleration and two meters of global SLR by the year 2100. The curves in Figure 21 can be approximated by:

$$E(t) = at + bt^2; \quad (\text{Equation 2})$$

where E is the predicted amount of SLR (in meters) at a future time t (the number of years from the baseline year 1992), a is the observed rate of SLR (1.7 millimeters/year), and b is an acceleration coefficient Paris et al. (2012). The acceleration coefficients are listed in Table 4.

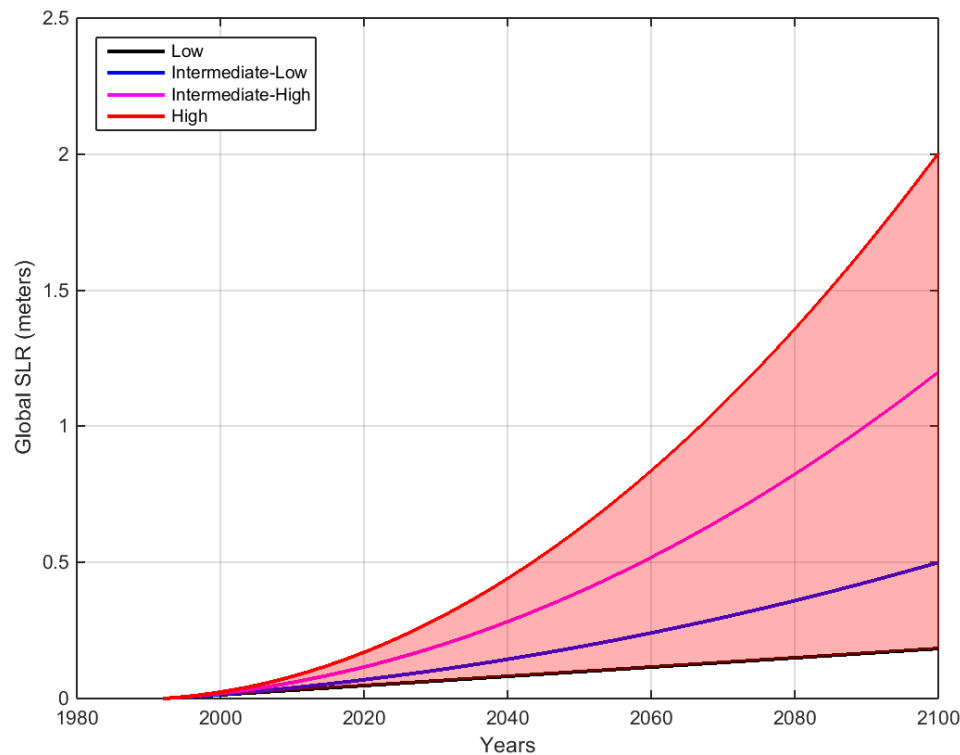


Figure 21. Future global SLR projections developed by Paris et al. (2012). There are four different scenarios which vary based on global greenhouse gas emissions: Low, Intermediate-Low, Intermediate-High, and High. The year 1992 is the baseline year.

Table 4. Acceleration Coefficients (b) for Future Sea Level Rise Scenario Curves from Paris et al. (2012).

SLR Scenario	Acceleration Coefficient (b)
Low (observed)	0
Intermediate-Low	2.71×10^{-5}
Intermediate-High	8.71×10^{-5}
High	1.56×10^{-4}

2.5.1 Relative Sea Level Rise

SLR occurs at different rates across the globe due to regional oceanographic effects and vertical land motion, including both subsidence and uplift (Paris et al. 2012; Zervas et al. 2013; Sweet et al. 2017). Therefore it is critical to adjust future SLR predictions based on local processes to calculate the future relative SLR in each area of interest. To do this, Compass followed the procedure recommended by Zervas et al. (2013) and replaced the observed global rate of SLR in Equation 1 ($a = 1.7$ millimeters/year)



with the observed rate of SLR at NOAA tide gauges within each site. Table 5 lists the observed rates of SLR.

Table 5. Observed Rates of SLR from Tide Gauges for Determining Future Relative SLR

NOAA Tide Gauge	Observed Rate of SLR - Value of a (millimeters/year)
Global	1.70
NOAA Station #8449130 Nantucket, Massachusetts	3.57

Notes: 1 – Data available at <https://tidesandcurrents.noaa.gov/sltrends/sltrends.html/>

Using the observed rate of SLR at each tide gauge accounts for regional oceanographic effects and local vertical land motion. Figure 22 shows an example of the relative SLR projections for a section of the coastline from Westerly to Charleston, Rhode Island.

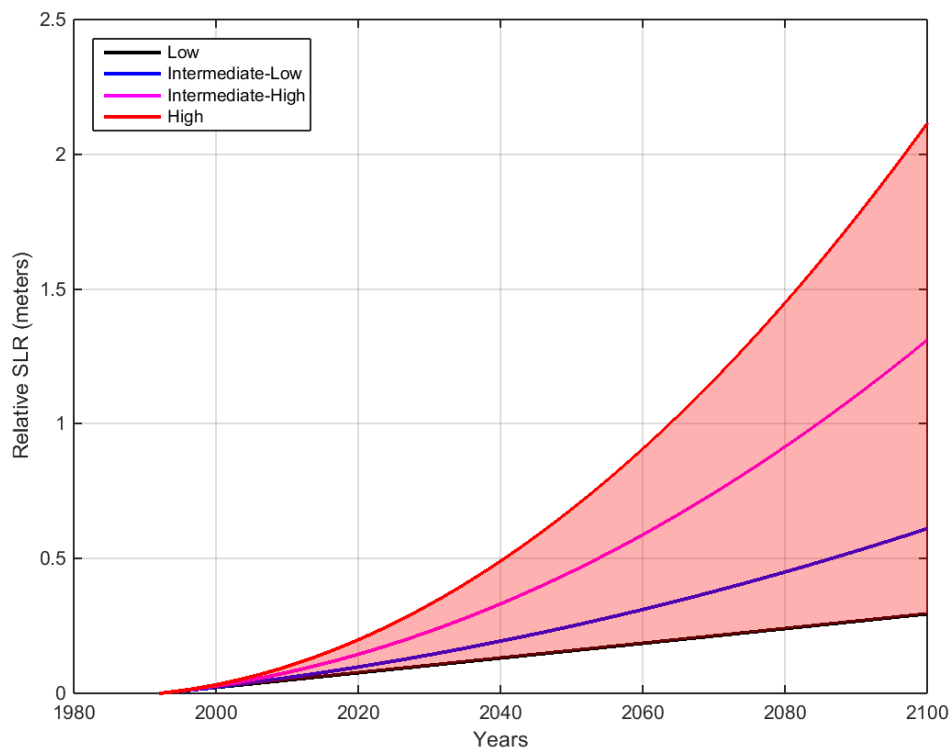


Figure 22. An example of relative SLR projections for a section of coastline from Westerly to Charleston, Rhode Island. The projections are the global SLR projections from Paris et al. (2012) adjusted for local effects with the observed SLR at the NOAA Newport, Rhode Island tide gauge. The projections use the year 1992 as a baseline year.



To predict future shoreline change, Compass further had to adjust the relative SLR projections for the baseline year of the Pilot Study: 2010. The Paris et al. (2012) SLR projections are based on the year 1992, while topographic data, shoretype classification, and NPFs in the Pilot Study are based on the year 2010. To calculate the predicted SLR between specific years, Equation 1 is modified as:

$$E(t_2) - E(t_1) = a(t_2 - t_1) + b(t_2^2 - t_1^2); \quad (\text{Equation 3})$$

where t_1 is the difference in years between the Pilot Study baseline year 2010 and 1992, and t_2 is the difference in years between the future year of interest (2030, 2050, or 2100) and 1992 (Paris et al. 2012). Predicted future amounts of SLR at each site for all scenarios and future timeframes are shown in Table 6.

Table 6. Predicted Relative Future SLR at Each Site for all Pilot Study Timeframes

County	SLR Scenario	SLR by Year (meters)		
		2030	2050	2100
Nantucket	Low (observed)	0.1	0.1	0.3
	Intermediate-Low	0.1	0.2	0.6
	Intermediate-High	0.2	0.4	1.3
	High	0.2	0.6	2.1

Notes: Relative future SLR predictions are based on the year 2010, which is the year of the airborne topographic LIDAR survey data and the baseline year for all future shoreline change predictions. They are slightly less than the SLR curves presented in (Figure 22) because those are based on the year 1992.

2.5.2 Future Sea Level Rise Factors

Future shoreline change will be dependent on the degree of acceleration of SLR. The Intermediate-Low, Intermediate-High, and High SLR scenarios all predict that SLR will speed up in future decades. These scenarios will successively cause more erosion than the Low SLR scenario, which simply assumes that sea levels will increase at the same rate as has been observed over the past several decades. To quantify the acceleration in future SLR projections, Compass followed the technical approach developed in the FEMA Region IX Sea Level Rise Pilot Study (BakerAECOM 2016). In this approach, an average rate of SLR is calculated between the year of interest and 2010 (Figure 23). The ratio of this rate to the observed SLR rate is then calculated. This can be simply expressed as:

$$F = l/b; \quad (\text{Equation 4})$$

where F is the factor of increase, l is the average rate of SLR between the year of interest and 2010, and b is same observed rates of SLR from Equations 1 and 2. For example, the predicted average rate of SLR for the High scenario at Site 3 to the year 2100 is 21.42 millimeters/year. The observed rate of SLR at the tide gauge is 1.76 millimeters/year (Table 5). The factor of increase is then $F = 21.42/1.76 = 12.2$. The



calculated factors are listed in Table 7. For the Low SLR projections, F equals 1.00. This means that there is no future increase in the rate of SLR.

It is important to note that although the SLR projections begin in the year 1992, the future predictions of SLR increase from the year 2010 for each scenario are valid. These predictions are valid even though there are differences in the starting SLR elevations at the year 2010 (Figure 21, Figure 22, and Figure 23). This is because we calculated the relative increase in SLR rate starting in the year 2010 within each scenario, and did not compare between scenarios.

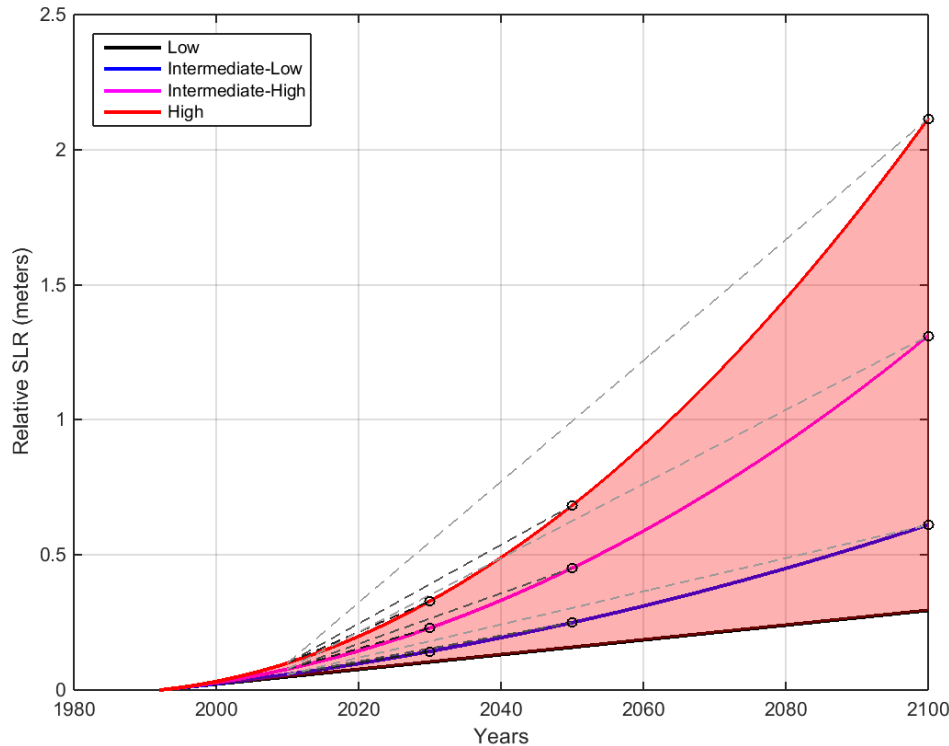


Figure 23. An example of how the SLR factors (F) are calculated for the stretch of coast from Westerly to Charleston, Rhode Island. The average rates of SLR are calculated between each year of interest (2030, 2050, and 2100) and the year 2010 (grey lines). The ratios between these years and the observed rates of SLR at each tide gauge are then calculated.

**Table 7.** Calculated Factors of Increase in Future SLR Rates Relative to Observed SLR Rates.

County	SLR Scenario	SLR by Year (meters)		
		2030	2050	2100
Nantucket	Low (observed)	1.00	1.00	1.00
	Intermediate-Low	1.43	1.58	1.96
	Intermediate-High	2.37	2.85	4.07
	High	3.45	4.32	6.51

Notes: Factor of 1.00 for the Low SLR scenarios indicates no increase in the SLR rate.

2.6 Future Erosion Calculations

Compass used the relative future increases in the rate of SLR, factor F from the previous section, to adjust historical shoreline change rates to future shoreline change rates. The following sections describe the specific calculations at sandy dunes and beaches (Section 2.6.1), coastal bluffs (Section 2.6.2), and hybrid areas (Section 2.6.3).

2.6.1 Sandy Dunes and Beaches

To analyze the future response at sandy shorelines, including the dune and beach shoretypes, Compass followed a technical approach developed in the FEMA Region IX Sea Level Rise Pilot Study (BakerAECOM 2016). In this approach, the Bruun Rule was used adjust the historical erosion rates calculated at each transect (Figure 24) (Bruun 1962). The Bruun Rule predicts that over sufficient time, a sandy shoreline will erode in response to SLR and come into equilibrium. Sand will erode from the foreshore and backshore and be transported offshore along the active nearshore profile, which extends offshore to the depth of closure (DOC). The Bruun Rule predicts the inland retreat distance by projecting the specific amount of SLR inland along the Bruun slope, or the slope from the DOC to a point on the beach as:

$$R_B = SLR/s; \quad \text{(Equation 5)}$$

where R_B is the predicted inland retreat distance, SLR is the specified amount of SLR, and s is the Bruun slope. The DOC and Bruun slope are discussed in more detail in Section 2.6.4.

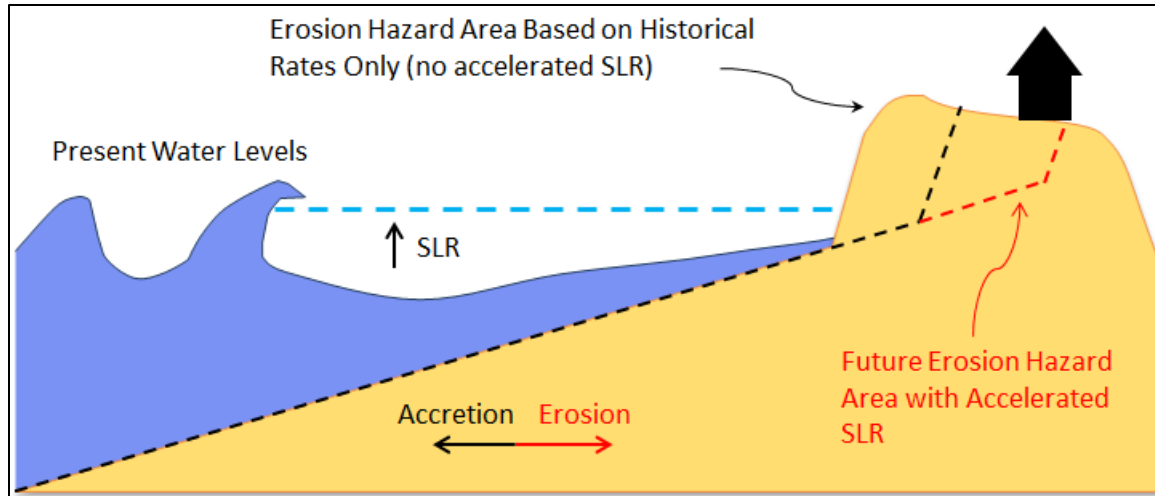


Figure 24. A conceptual sketch of the predicted future erosion response at sandy dune and beach transects.

Instead of simply projecting a future retreat distance along the Bruun slope, BakerAECOM (2016) used the Bruun Rule to calculate a more detailed erosion response. BakerAECOM (2016) assumed that SLR has been affecting sandy shorelines for decades, which is evidenced by observed SLR in tide gauge records dating back to the mid-1800's. BakerAECOM (2016) further assumed that the historical rates of shoreline change are due both to observed SLR, which works to erode beaches, and nearshore coastal process, which can either erode or prograde beaches. The Bruun Rule was applied with the observed rates of SLR from tide gauges to determine the historical erosion rates that would have been observed in the absence of other nearshore coastal processes. These historical erosion rates due to SLR were then subtracted from the actual historical shoreline change rates to estimate the shoreline change rates due to nearshore coastal process. Finally, BakerAECOM (2016) assumed that the rates of change due to nearshore processes would remain constant in the future while the rates of change to SLR would increase. The shoreline change rates due to SLR were increased by the future SLR factors to increase the fraction of shoreline change due to SLR. This approach is summarized in the following steps.

Compass first assumed that the historical rates of shoreline change were a combination of two components:

$$r_h = r_{coastal} + r_{h,SLR}; \quad (\text{Equation 6})$$

where r_h is the LRR calculated at each sandy beach transect, $r_{coastal}$ is the amount of the historical shoreline change rate due to nearshore coastal processes, and $r_{h,SLR}$ is the amount of the historical shoreline change rate due to observed rates of SLR at each tide gauge. The subscript " h " stands for historical. Predicted future rates (r_f) are then:

$$r_f = r_{coastal} + r_{f,SLR}; \quad (\text{Equation 7})$$

which is a combination of the shoreline change rate due to nearshore coastal processes, assumed to be the same in the future, and the rate of shoreline change to do future SLR ($r_{f,SLR}$).

To estimate $r_{h,SLR}$, the Bruun Rule was applied:

$$r_{h,SLR} = \frac{b}{s}; \quad (\text{Equation 8})$$



with b as the observed rate of SLR from a tide gauge and s as the Bruun slope. The shoreline change rate due to nearshore coastal processes was then calculated by re-arranging Equation 5:

$$r_{coastal} = r_h - r_{h,SLR}. \quad (\text{Equation 9})$$

The future rate of shoreline change due to SLR was estimated by increasing the historical rate of shoreline change due to SLR and scaling by F for a particular timeframe and SLR scenario

$$r_{f,SLR} = r_{h,SLR} \times F. \quad (\text{Equation 10})$$

Values of F for each timeframe and SLR scenario are found in Table 7. The predicted future retreat distances for a particular SLR scenario and timeframe were then found by multiplying the rate by time:

$$R_f = r_f \times t. \quad (\text{Equation 11})$$

It is important to highlight that this approach preserves the historical trends in shoreline change due to nearshore coastal processes. For example, if a beach has historically prograded, the predicted future erosion response may not be large, because SLR will be working against the processes that have caused accretion. If a beach has historically eroded, the predicted future erosion response might be large as SLR will be combining with the processes that have caused erosion.

2.6.2 Coastal Bluffs

Coastal bluff erosion is a complex process, due to combinations of marine and terrestrial process that can vary from site to site. Although it is generally expected that bluffs will erode due to future SLR, there is no clear scientific consensus on exactly how rapidly they will erode. To analyze the future response at coastal bluffs, Compass also followed a simplified technical approach developed in the FEMA Region IX Sea Level Rise Pilot Study (BakerAECOM 2016). This was different than the technical approach applied at sandy beaches because coastal bluffs only erode while sandy beaches can erode or prograde (Figure 25). The approach assumes that historical bluff erosion is solely due to observed SLR:

$$r_h = r_{h,SLR}; \quad (\text{Equation 12})$$

such that $r_{h,SLR}$ is equal to the LRR calculated at a particular transect. There are no field observations to directly support this assumption; however, there are several numerical modelling studies that suggest a strong, direct correlation between bluff erosion and SLR (Walkden and Dickson 2006; Walkden and Dickson 2008; Ashton et al. 2011) The future erosion rate is then increased by the SLR increase factor F raised to a power of 0.5:

$$r_f = r_{h,SLR} \times F^{0.5}. \quad (\text{Equation 13})$$

This is based on a model of coastal bluff erosion developed by Ashton et al. (2011). The model assumes that unlike sandy shorelines, coastal bluffs can withstand some wave attack and erode more slowly. The predicted future retreat distance is then simply the future erosion rate multiplied by the time period of interest.

$$R_f = r_f * t \quad (\text{Equation 14})$$

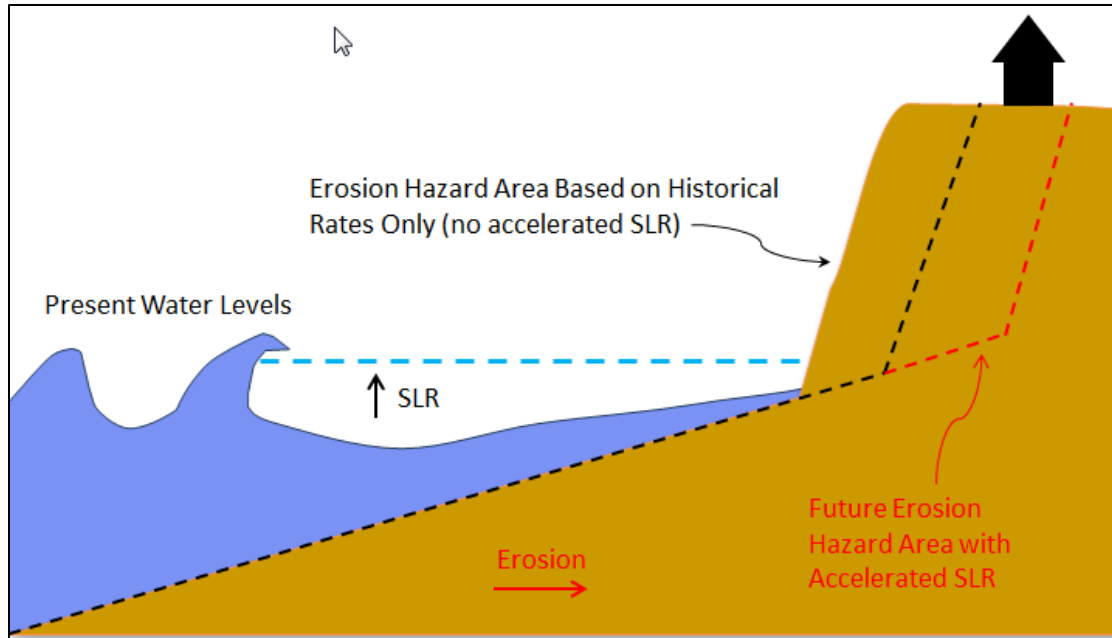


Figure 25. A conceptual sketch of the predicted future erosion response at coastal bluffs.

2.6.3 Hybrid Areas – Sandy Beaches Backed by Coastal Bluffs

Several sections of the coastline in this county consist of sandy beaches backed by tall coastal bluffs. The beaches are expected to erode due to future SLR, and for larger SLR scenarios (Intermediate-High and High) over longer timeframes (2100), the backing coastal bluffs are also predicted to erode (Figure 26).

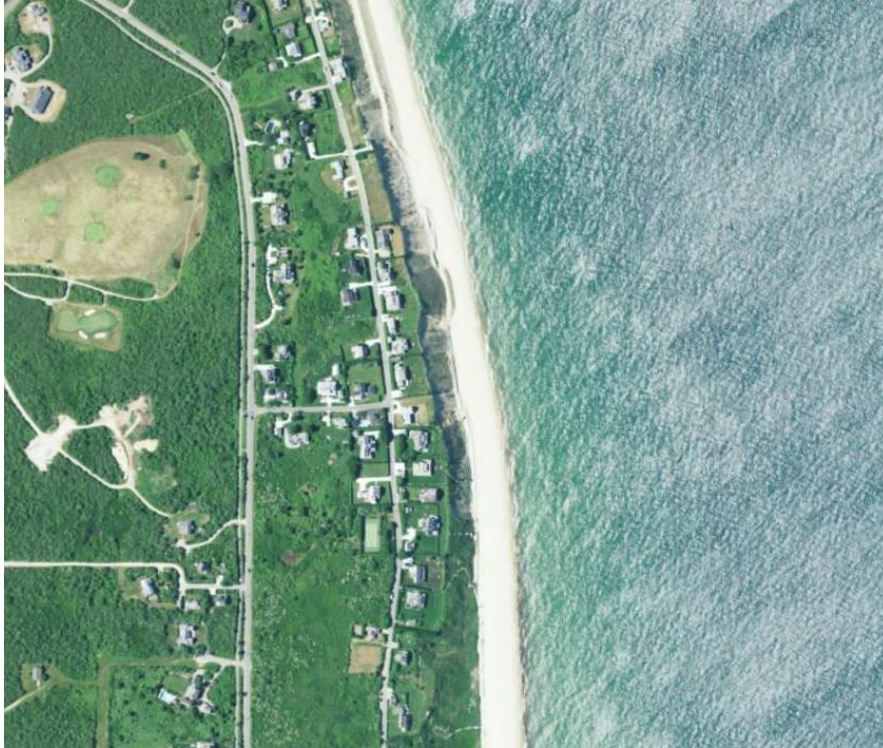


Figure 26. An example of a wide sandy beach backed by a coastal bluff at Siasconset, on the eastern shore of Nantucket, Massachusetts. The aerial photos shows that bluffs to the north are rapidly eroding. The bluffs to the south have historically been stable, although the beach is eroding. The photo shows these bluffs are well vegetated with trails and paths. Future erosion predictions for high SLR scenarios and long timeframes demonstrate that the historically stable bluffs might erode. Compass applied a hybrid analysis approach for these areas.

For each particular SLR scenario and timeframe, the rate of sandy beach erosion was projected in times steps inland along the transect (Equations 6-11) until erosion reached the bluff edge. For the remaining time steps in the future projection, a bluff erosion rate was projected landward (Equations 12-14).

Predictions of future bluff erosion require a bluff erosion rate (LRR) and at these sites there were no bluff erosion rates as the bluffs were historically stable. Therefore, Compass applied the average bluff erosion rate from adjacent reaches, which typically had similar bluff geometries and geomorphologies, to the predictions of future bluff erosion within the hybrid beach and bluff areas.

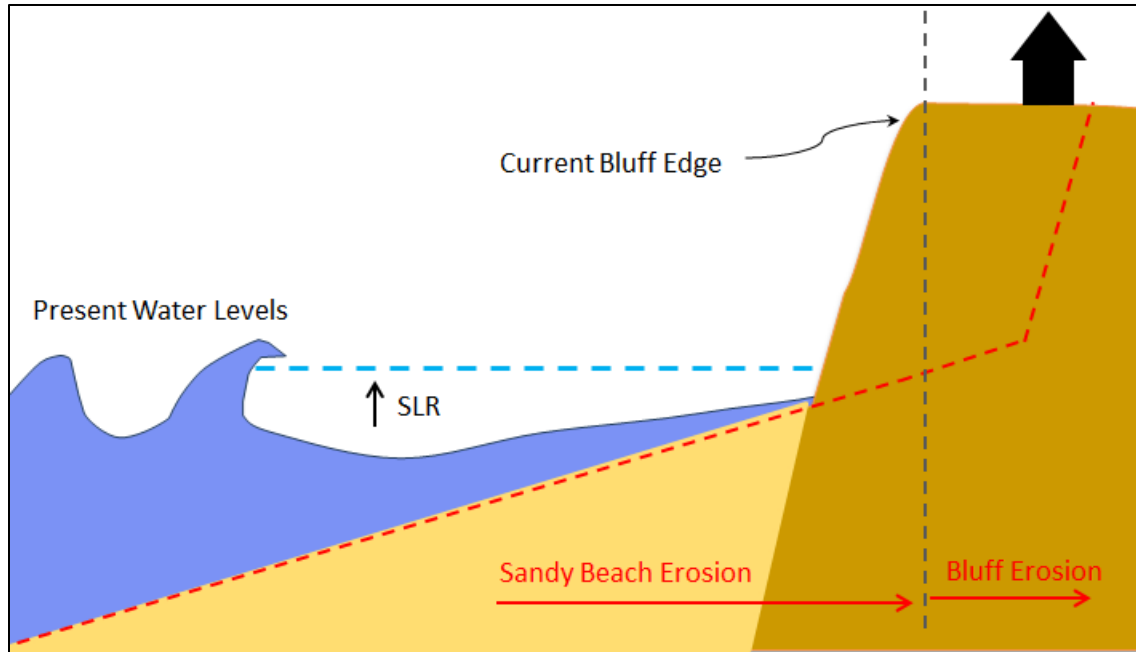


Figure 27. A conceptual diagram of the hybrid approach applied at eroding sandy beaches backed by stable coastal bluffs that are predicted to erode in the future. For each particular SLR scenario and timeframe, sandy beach erosion was projected inland. The sandy beach erosion was projected in time steps and if the beach erosion projected to the bluff edge, bluff erosion was projected landward for the remainder of the timeframe.

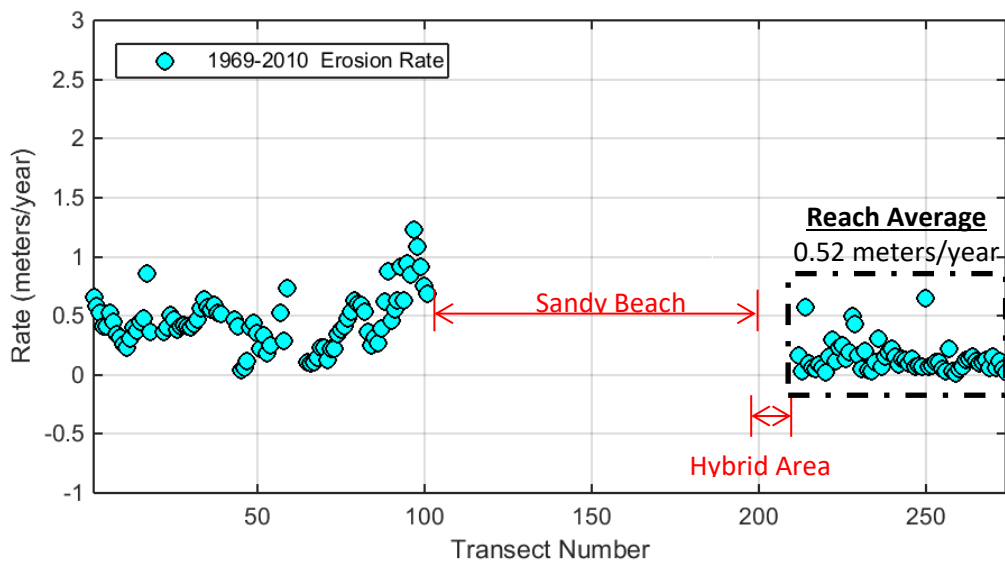


Figure 28. An example of historical bluff erosion rates (LRRs) for transects in Nantucket, Massachusetts. There are no historical bluff erosion rates for the southern bluffs at Siasconset (Hybrid Area - Transects 200-213); however, there are relatively consistent bluff erosion rates for north Siasconset (Transects 213-275). Compass averaged the bluff erosion rates within this adjacent reach (0.52 meters/year) and applied this average rate to the hybrid area.



2.6.4 The Bruun Slope

To estimate the future erosion response due to SLR, Compass applied a modified Bruun Rule as detailed in Section 2.6.1. A conceptual diagram of the Bruun Rule is shown in Figure 29. The Bruun slope (s) is the active nearshore profile slope between the DOC and the foreshore or backshore of the beach. Compass selected MHHW as the landward endpoint as this point is within the active profile range (Table 3).

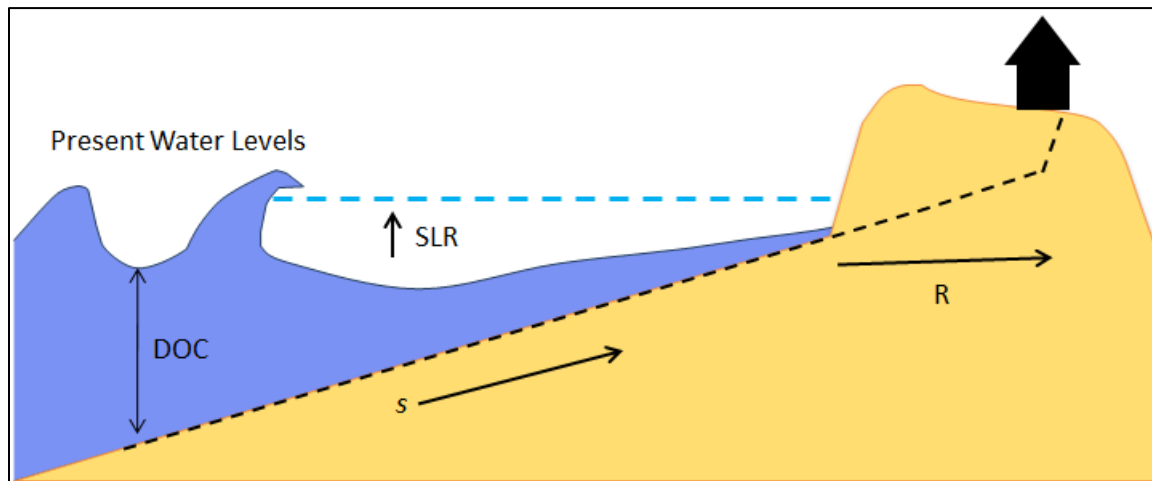


Figure 29. A conceptual diagram of how the Bruun Rule is typically applied with the Bruun slope (s) to the DOC. The predicted retreat distance (R) is determined by projecting the future amount of SLR landward along s .

The two critical technical components of the Bruun slope calculation are 1) the calculation of the DOC; and 2) the calculation of the resulting Bruun Slope. There are many ways to calculate the DOC, which is the deepest depth of cross-shore sediment transport (Hallermeier 1981; Brutsche et al. 2015). As wave energy typically transports sediment offshore, empirical equations are dependent upon characteristic wave heights, wave periods, and sediment characteristics (Hallermeier 1981). Simplified empirical equations are dependent on wave height and wave period only. In the Pilot Study, Compass tested out several equations and determined that calculation of an offshore DOC is best suited to this study. Hallermeier (1978) developed an equation to calculate an outer (more offshore) depth of closure as:

$$DOC = 2\overline{H_s} + 11\sigma_s. \quad (\text{Equation 15})$$

where $\overline{H_s}$ is the annual mean significant wave height and σ_s is the standard deviation of the significant wave height. Compass calculated the DOC for different areas of the coast based on publicly available wave data available for each particular area. Wave data sources included the NOAA NDBC and the USACE Wave Information Studies (WIS) program (<http://wis.usace.army.mil/>).

In the Pilot Study, Compass tested out different methods to calculate the Bruun slope with one specific DOC on variety of cross-shore profiles (Figure 30). This calculation is not necessarily straightforward along cross-shore profiles with sand bars such that there are multiple locations for the DOC. Compass ultimately applied a technique consisting of projecting lines with a range of slopes offshore from MHHW to the DOC. The error between each projected slope and the cross-shore profile is calculated as:

$$\varepsilon = \frac{\sum (z - z_s)^2}{\sum z^2}; \quad (\text{Equation 18})$$



where ϵ is the error, z is each cross-shore profile elevation, and z_s is each elevation along a line with the specified slope. The slope that minimized the error was selected as the best-fit slope. An example of a best fit slope is also shown in Figure 30.

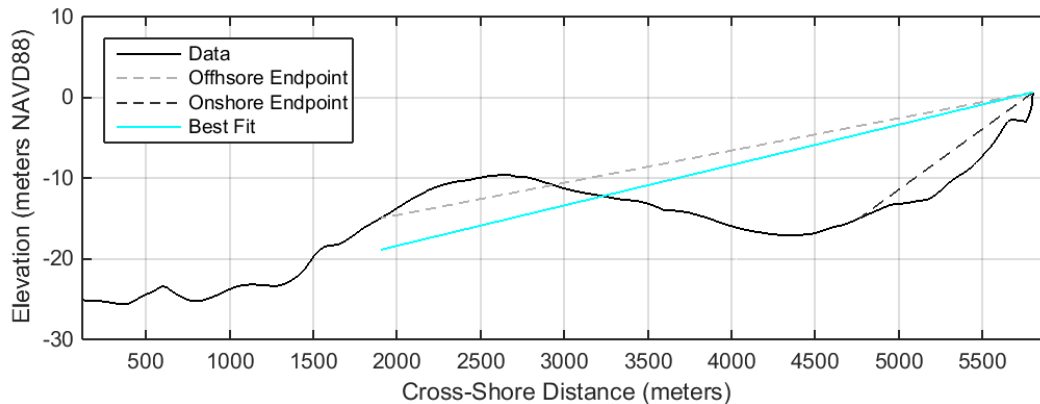


Figure 30. An example of a cross-shore profile that reaches the DOC of -15 meters NAVD88 in two offshore locations, due to the presence of an offshore sand bar. The average “offshore slope” is relatively flat and the average “onshore slope” is relatively steep. Compass used a best-fit slope, which more accurately captures the overall profile slope and is not as sensitive to the presence of offshore bars.

2.7 Field Site Visits

Compass conducted field site visits along the shoreline of Nantucket on September 18 - 19, 2017. Field site visits were used to confirm identified shoretypes (dunes, beaches, bluffs). Field staff collected global positioning data (GPS) of NPFs along transect lines (Figure 31). Because of the time difference between the field site visits in 2017 and the topographic LiDAR survey in 2010, there were areas where the locations of the NPFs identified in the field did not exactly match the locations of the NPFs identified in the data. However, the GPS data gave Compass a point of reference to use when analyzing the 2010 data. Field visits were also used to visually confirm high calculated historical erosion and accretion rates (LRRs). Beaches and bluffs that have historically eroded rapidly show evidence of erosion including scarps, lack of vegetation, bluff collapse, etc. Beaches that have historically accreted rapidly tend to be wide and flat. This visits provided a qualitative check on the calculated rates.



Figure 31. Compass conducted field site visits at Nantucket, Massachusetts from September 18 – 19, 2017.



03 Results

Compass developed maps of future erosion hazard areas for the Low, Intermediate-Low, Intermediate-High, and High SLR scenarios to the years 2030, 2050, and 2100. This section describes the analysis results and maps.

3.1 Predicted Future Erosion

Predicted future erosion distances for all years and SLR scenarios were calculated and mapped. In general, predicted erosion distances increase with the magnitude of SLR (Low – High) and the length of time (2030 – 2050). The alongshore variability also increases with longer timeframes, with the predictions for 2100 having the largest amount of alongshore variability. This is because small differences between transects in future erosion rates become magnified over a 90 year timeframe (2010 to 2100). Large coastal erosion hazard areas were predicted in areas that have seen rapid erosion (have high LRRs). Along beaches that have historically accreted, some accretion was still predicted for lower SLR scenarios and shorter timeframes. For higher SLR scenarios and longer timeframes, some erosion was predicted.

Figure 32 shows an example of the predicted future coastal erosion hazard areas for the south coast of Nantucket Island, an area which has historically eroded rapidly. The future hazard zones for the years 2030, 2050, and 2100 under the Intermediate-High SLR scenario indicate that this could be a high erosion area in the future. The results also indicate high future erosion at Siasconset on the western coast of the island and the bluff and dune-backed beaches along the northeastern shore of the island. Some wide sandy beaches, including Surfside Beach and the northern section of Tom Nevers Beach, have historically accreted. At these beaches, the results indicate that the beaches will continue to accrete or remain stable under lower SLR scenarios and shorter timeframes. Under higher SLR scenarios and longer timeframes, these beaches will begin to erode.

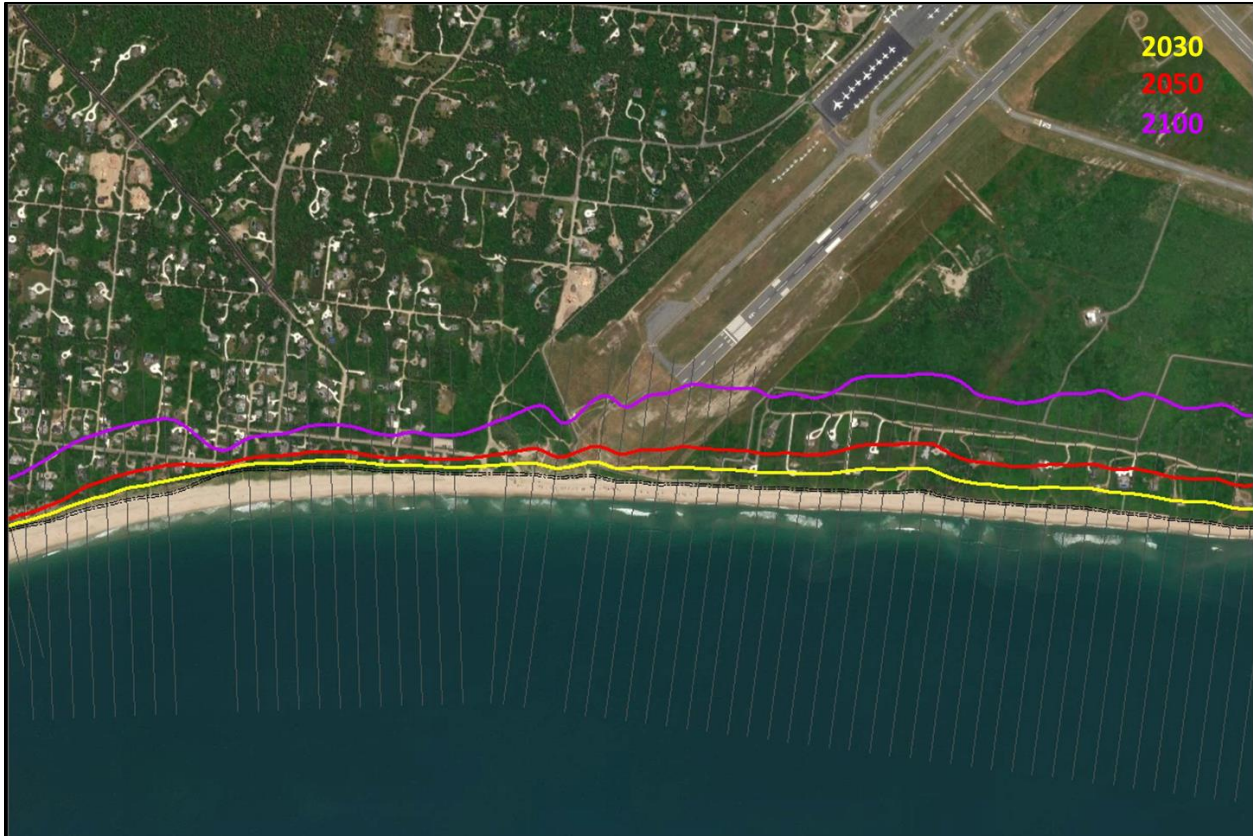
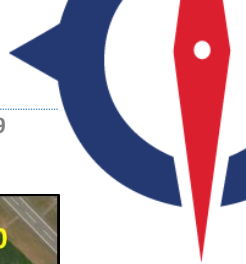


Figure 32. The predicted future erosion distances under the Intermediate-High SLR scenario for the years 2030 (in yellow), 2050 (in red), and 2100 (in purple) along the south coast of Nantucket Island, near the airport.

3.2 Coastal Erosion Hazard Area Maps

Compass created GIS shapefile data of the predicted future coastal erosion distances. Coastal erosion hazard area maps were created for the Intermediate-High SLR scenarios (Figure 33) for the years 2030, 2050, and 2100. The Intermediate-High SLR scenario was selected for mapping as it covers a range of specific SLR increments over the specified timeframes (Figure 21). This range, combined with the three future timeframes, provides coastal communities with a variety of hazard area boundaries to meet the needs of different community members. Homeowners, with typical 30 year mortgages, can use the mapped future coastal erosion hazard areas for the years 2030 or 2050 to understand how their properties might be impacted. Community planners can use the mapped future coastal erosion hazard areas for 2100 to plan long-term mitigation strategies.

A GIS geodatabase (GDB) was created including the mapped erosion hazard areas from the Intermediate-High SLR scenario and the additional erosion hazard area boundaries for the remaining SLR scenarios (Low, Intermediate-Low, and High).

For complete results it is recommended that the full of set of maps be reviewed.

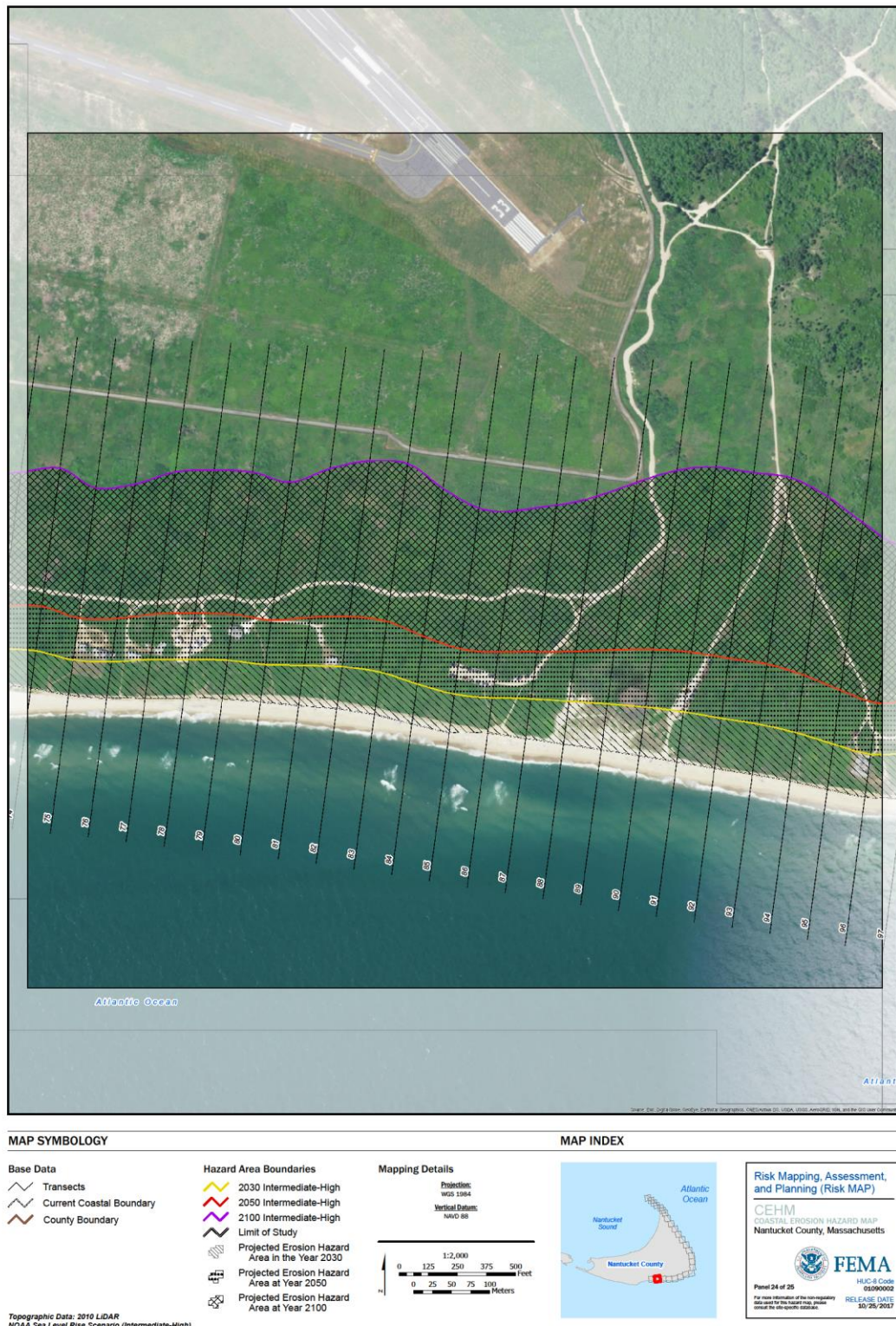


Figure 33. An example of the mapped Intermediate-High SLR erosion scenarios for the southern shore of Nantucket, Massachusetts. Coastal erosion hazard areas are mapped for the years 2030, 2050, and 2100. Historically, the bluffs in this area have eroded rapidly.



3.3 Mapping

Some modifications were made to the erosion hazard area boundaries during the mapping process in GIS. These are described in this section.

Removal of Results at Certain Shoreline Protection Structures: During the Pilot Study it was found that certain coastal protection structures significantly altered historical erosion rates and the future erosion predictions. In many cases, an erosion protection structure had been placed in a particular high erosion area mid-way through the historical period of record. This resulted in the calculation of an intermediate historical erosion rate that was not reflective of either the high erosion environment prior to construction of the structure or the low erosion environment after construction of the structure. Subsequently, the calculations often predicted intermediate erosion distances that were not reflective of the either low erosion environment with the structure being well-maintained until 2100 or the high erosion environment with the structure failing or being removed. Ultimately, to incorporate each structure into the analysis would require knowledge of the structures future performance under future SLR and maintenance, both of which are unknown and beyond the scope of this study. Therefore, mapping modifications were made. An example is shown in Figure 34. Essentially, the results at each identified structure were removed and the hazard areas were interpolated across the predicted area. This created a hazard area that reflects the future unprotected scenario and assumes the structures future performance is uncertain or unknown. It also assumes that the future erosion hazard area is the same as the adjacent, unprotected sections of coast, which have the same exposure and geomorphology. Considering that the goal of the project is to identify areas that are at risk due to future SLR this mapping approach is justified.

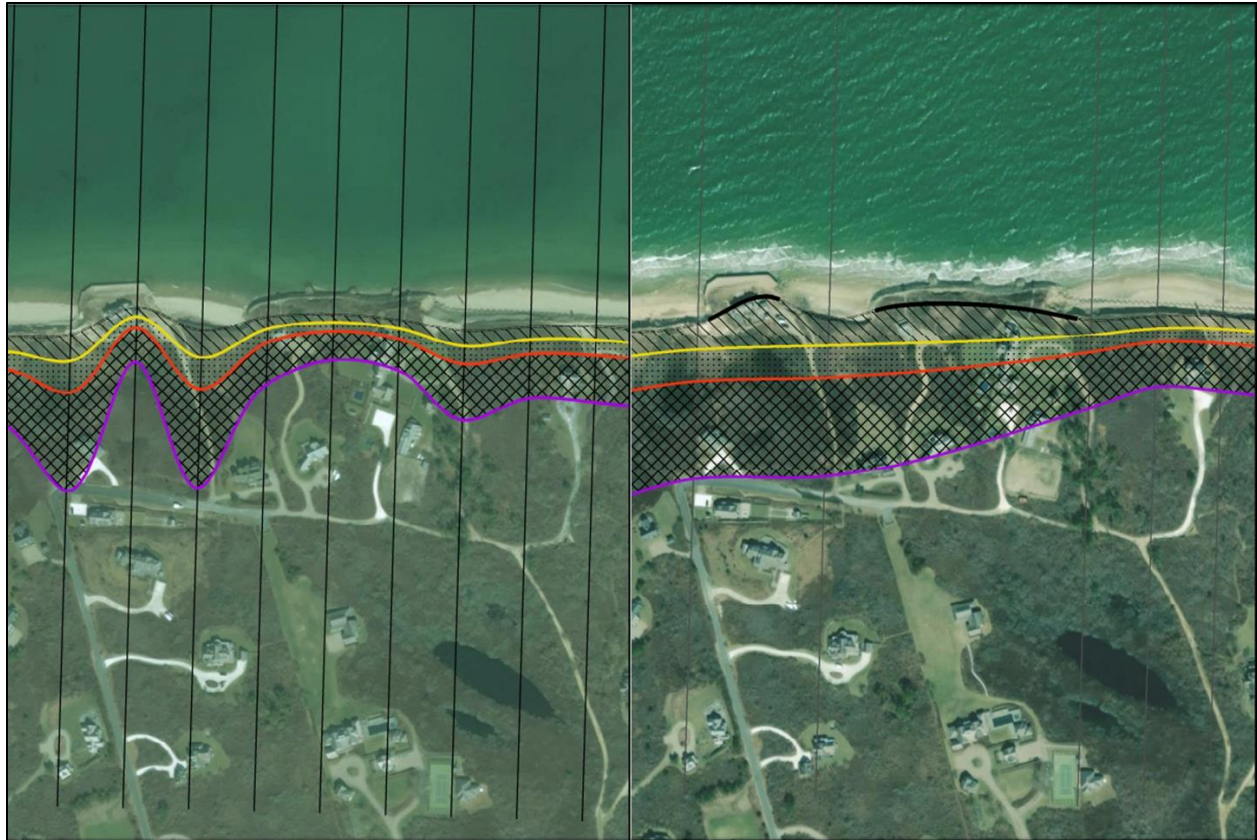


Figure 34. An example of an area where the future erosion predictions were modified in mapping at a coastal protection structure. The left panel shows two coastal protection structures that have impacted the calculation of historical erosion rates and ultimately the prediction of future erosion hazard areas (shown as hatched areas with colored boundaries). Both the historical erosion rates and the future hazard areas are not representative of the coastal geomorphology of the area or the risk posed by future SLR. The right panel shows the mapping technique in which the results at these transects are removed, the hazard areas are interpolated across the protected area, and the Current Coastal Boundary line is highlighted by a black line, indicating the presence of a structure.

Alongshore Smoothing –In the Pilot Study, Compass found that the predicted erosion distances can be variable in the alongshore due to small differences in historical erosion rates, particularly with future erosion predictions over longer time periods like 2100. As the response to future SLR should be somewhat similar over reaches with similar exposure and coastal geomorphology, Compass applied an alongshore moving average to the results, applied over every three transects. This was used to preserve the overall trends in future erosion and smooth out some of the variability over short length scales.

04 Summary and General Recommendations

Compass completed a Study in Nantucket County to predict future coastal erosion hazard areas due to SLR within FEMA Region I. This Study meets a critical need for coastal communities to understand the risk they will face in coming decades and plan for resilience. The Study also meets several agency objectives, including those set forth by FEMA, FIMA, and TMAC.

The coastal erosion maps were presented to key stakeholders from Nantucket County during an outreach meeting conducted in June 2018. The meeting was conducted to ensure the community



members understand the value of the maps and how they can be used. Further community outreach can help different stakeholders begin to plan mitigation actions and reduce their risk.

Compass mapped future coastal erosion hazard areas for several specific timeframes: the years 2030, 2050, and 2100. These timeframes were adopted to be useful to different community members, ranging from homeowner to community planners.

As with other coastal flood risk products, Compass recommends that the coastal erosion hazard maps be updated at regular intervals in the future, ideally every 15 years. Currently, there is still uncertainty and a large range in future climate change scenarios and SLR projections. In future decades, more observations will allow these SLR projections to be refined. Regular updates to the maps will improve accuracy.



05 References

- AECOM 2013. Lake Ontario Pilot Study Memorandum for New York State Offices for General Services and New York Department of Environmental Conservation, Technical Report, 36pp.
- Ashton, A.D., Walkden, M.J.A., and Dickson, M.E. 2011. Equilibrium responses of cliffed coasts to changes in the rate of sea level rise. *Marine Geology*, v284, 217-229.
- BakerAECOM 2016. FEMA Region IX Sea Level Rise Pilot Study: Future Conditions Analysis and Mapping, San Francisco Bay, California, Technical Report, 100pp.
- Brutsche, K.E., Rosati III, J., and Pollock, C.E. 2015. Calculating Depth of Closure Using WIS Hindcast Data, US Army Corps of Engineers, Technical Report (ERC/CHL CHETN-VI-XX), 11pp.
- Birkemeier, W.A. 1985. Field data on seaward limit of profile change. *Journal of Waterway, Port, Coastal and Ocean Engineering*, v111, 598-602.
- Bruun, P. 1962. Sea level rise as a cause of shore erosion, American Society of Civil Engineers Proceedings, *Journal Waterways and Harbors Division*, v88, 117-130.
- Compass 2017. FEMA Region I Coastal Erosion Pilot Study, Technical Report, 60pp.
- Crowell, M. and Leatherman, S.P. 1999. Coastal erosion mapping and management, *Journal of Coastal Research*, v14 (Special Issue), 196pp.
- Crowell, M., Douglas, B.C., Leatherman, S.P. 1997. On forecasting future U.S. shoreline positions: A test of algorithms, *Journal of Coastal Research*, v14, 1245-1255.
- Crowell, M., Leatherman, S.P., and Buckley, M.K. 1993. Shoreline change rate analysis: Long term versus short term data, *Shore and Beach*, v14, 13-20.
- Hallermeier, R.J. 1981. A profile zonation for seasonal sand beaches from wave climate, *Coastal Engineering*, v4, 253-277.
- Hallermeier, R.J. 1978. Uses for a calculated limit depth to beach erosion. Proceedings, *Coastal Engineering*, 1493-1512.
- Hapke, C.J., Himmelstoss, E.A., Kratzmann, M.G., List, J.H., and Thieler, E.R. 2010. National Assessment of Shoreline Change: Historical Shoreline Change along the New England and Mid-Atlantic Coasts, technical report (USGS: OF2010-1118), 65pp.
- Heinz Center 2000. Evaluation of Erosion Hazards, The H. John Heinz Center for Science, Economics, and Management, Technical Report, 252pp.
- Nicholls, R.J., Birkemeier, W.A., and Lee, G. 1998. Evaluation of depth of closure using data from Duck, NC, USA, *Marine Geology*, v148, 179-201.
- Paris, A., Bromirski, P., Burkett, V., Cayan, D., Culver, M., Hall, J., Horton, R., Knuuti, K., Moss, R., Obeysekera, J., Sallenger, A., and Weiss, J. 2012. Global Sea Level Rise Scenarios for the U.S. National Climate Assessment, Technical Report (NOAA: OAR CPO-1), 33pp.
- Ranasinghe, R., Callaghan, D., and Stive, M.J.F. 2011. Estimating coastal recession due to sea level rise: beyond the Bruun rule, *Climatic Change*, v110, 561-574.
- Ruggiero, P. and List, J. 2009. Improving accuracy and statistical reliability of shoreline position and change rate estimates, *Journal of Coastal Research*, v25, 1069-1081.
- STARR II 2017. Future Sea Level Rise and Erosion Projection Assessment, Technical Report, 159pp.



- Stockdon, H.F., Sallenger, A.H., List, J.H., and Holman, R.A. 2002. Estimation of shoreline position from airborne topographic lidar data, *Journal of Coastal Research*, v18, 502-513.
- Stockdon, H.F., Holman, R.A., Howd, P.A., and Sallenger, A.H. 2006. Empirical parameterization of setup, swash, and runup, *Coastal Engineering*. v53. pp. 573-588.
- Sweet, W.V., Kopp, R.E., Weaver, C.P., Obeysekera, J., Horton, R.M., Thieler, E.R., and Zervas, C. 2017. Global and Regional Sea Level Rise Scenarios for the United States, Technical Report (NOAA: NOS CO-OPS 083), 75pp.
- TMAC 2015. Future Conditions: Risk Assessment and Modeling, Technical Report, 233pp.
- USACE 2002. Coastal Engineering Manual, Engineer Manual 1110-2-11000, US Army Corps of Engineers, Washington D.C. (6 Volumes).
- Walkden, M. and Dickson, M. 2006. The response of rock shore profiles to increased sea-level rise, Tyndall Centre for Climate Change Research, Technical Report, 22pp.
- Walkden, M. and Dickson, M. 2008. Equilibrium erosion of soft rock shores with a shallow or absent beach under increased sea level rise, *Marine Geology*, v251, 75-84.
- Weber, K.M., List, J.H., and Morgan, K.M 2005. An operational mean high water datum for determination of shoreline position from topographic lidar data: U.S. Geological Survey Open File Report 2005-1027, available at <https://pubs.usgs.gov/of/2005/1027/index.html>.
- Zervas, C., Gill, S., Sweet, W. 2013. Estimating Vertical Land Motion from Long-Term Tide Gauge Records, Technical Report (NOAA NOS: CO-OPS 065), 30pp.

